The Josephson-Anderson Relation and the Origin of Turbulent Drag

Gregory L. Eyink
The Johns Hopkins University

2022 Simons Collaboration on Wave Turbulence Annual Meeting
December 1, 2022

Thanks to the Simons Foundation, Targeted Grant in Mathematics & Physical Sciences - 663054

The D'Alembert Paradox

Jean le Rond d'Alembert
(1717-1783)

"It seems to me that the theory [potential flow], developed in all possible rigor, gives, at least in several cases, a strictly vanishing resistance, a singular paradox which I leave to future Geometers to elucidate…"

D'Alembert, submission for the 1749 Prize Problem of the Berlin Academy

This paradox was resolved by Saint-Venant (1846), who pointed out the importance of even a very small viscosity, which leads to a thin boundary layer, as further elaborated by Prandtl (1904) and others (see Stewartson (1981)).

The Modern D'Alembert Paradox

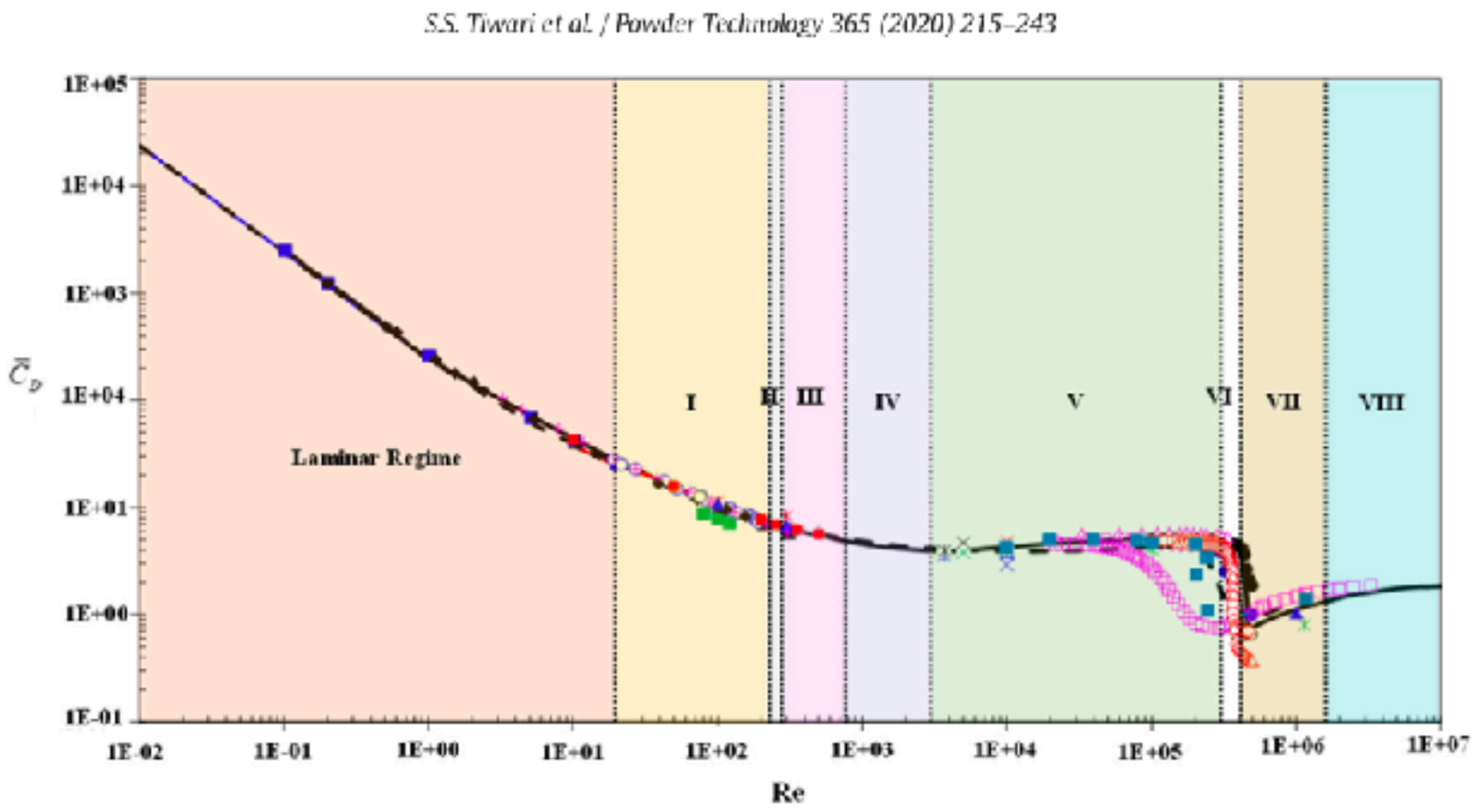

Drag coefficient of a stationary sphere

It appears that drag <u>does not vanish</u> in the limit $Re \to \infty$, but in that limit the solution of the Navier-Stokes equation tends to a (weak) Euler solution:

Theodore D Drivas and Huy Q Nguyen, "Remarks on the emergence of weak Euler solutions in the vanishing viscosity limit," Journal of Nonlinear Science 29, 709– 721 (2019)

An Experimental Puzzle on Anomalous Dissipation

PHYSICAL REVIEW E VOLUME 56, NUMBER 1 JULY 1997

Energy injection in closed turbulent flows: Stirring through boundary layers versus inertial stirring

O. Cadot,* Y. Couder, A. Daerr, S. Douady, and A. Tsinober†
Laboratoire Physique Statistique, Ecole Normale Supérieure, 24 rue Lhomond, 75231 Paris, France

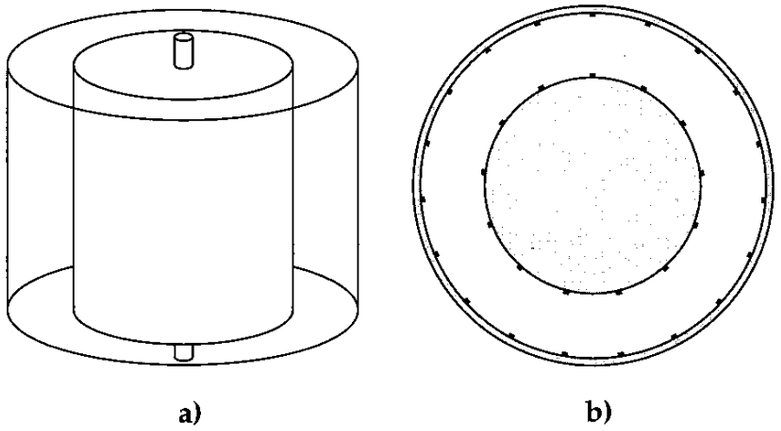

FIG. 4. Schemes of experiment B: (a) the Couette-Taylor cell with smooth surfaces and (b) the section of the system perpendicular to the axis of rotation and showing the ribs which make the walls rough.

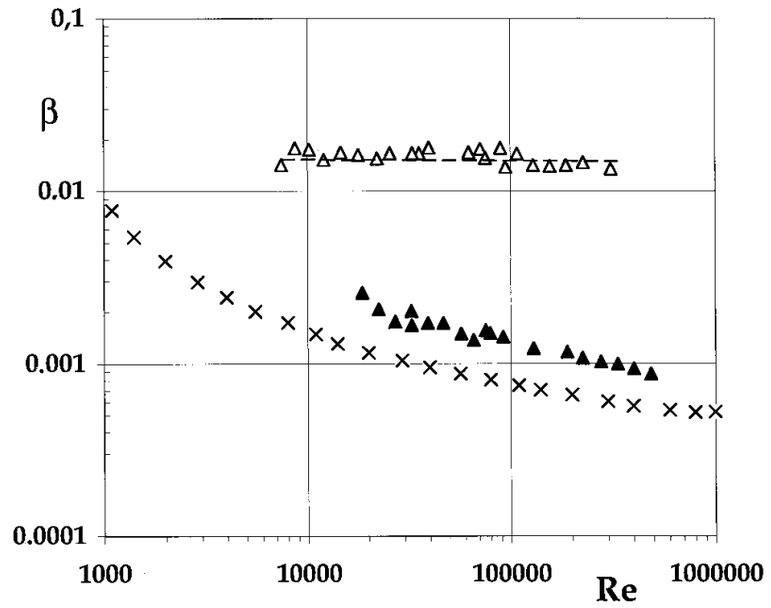

FIG. 5. Couette-Taylor experiments. Logarithmic plots of the nondimensional rates of energy dissipation β_D as a function of the Reynolds number. The black triangles (▲) are the results obtained with smooth cylinders, and the open ones (△) correspond to those obtained with the ribbed ones. The crosses (×) show for comparison the rates of energy injection β_D deduced from the data obtained with smooth cylinders by Lathrop, Finenberg, and Swinney [8].

strong anomaly: flow past a grid, jets through orifices, wakes behind bluff bodies such as cylinders and spheres

weak anomaly: pipe and channel (Poiseuille) flow, developing boundary layer over a flat plate, Taylor-Couette flow, von Kármán flow (or “French washing machine”), Rayleigh-Bénard turbulence…*except when the walls are rough!*

Polymer Drag Reduction

Toms, B. A. “Some observations on the flow of linear polymer solutions through straight tubes at large Reynolds number,” Proc First Int Congr on Rheol II:135– 141 (1948)

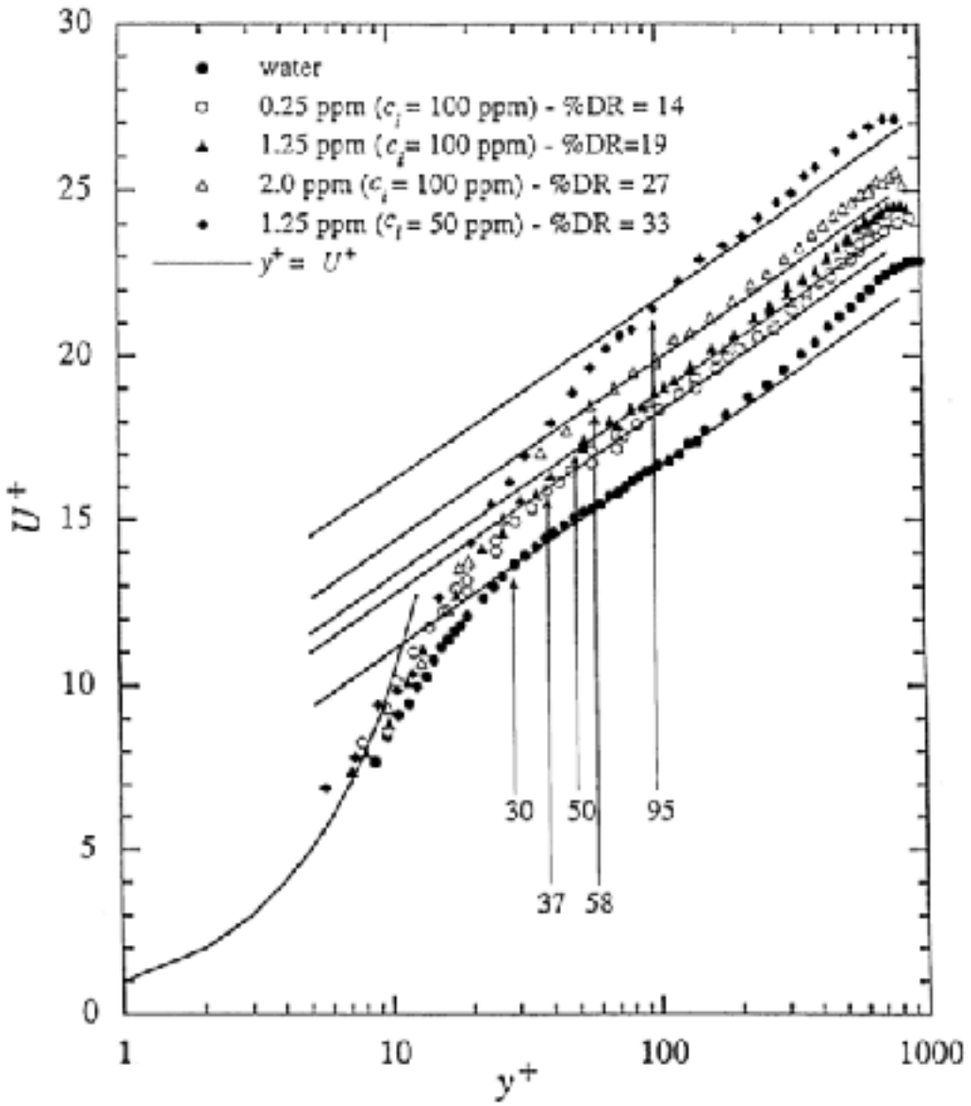

Fig. 3. Non-dimensional streamwise velocity, U^+, versus the non-dimensional distance from the wall, y^+ for low per cent drag reduction runs with best *log layer* fit

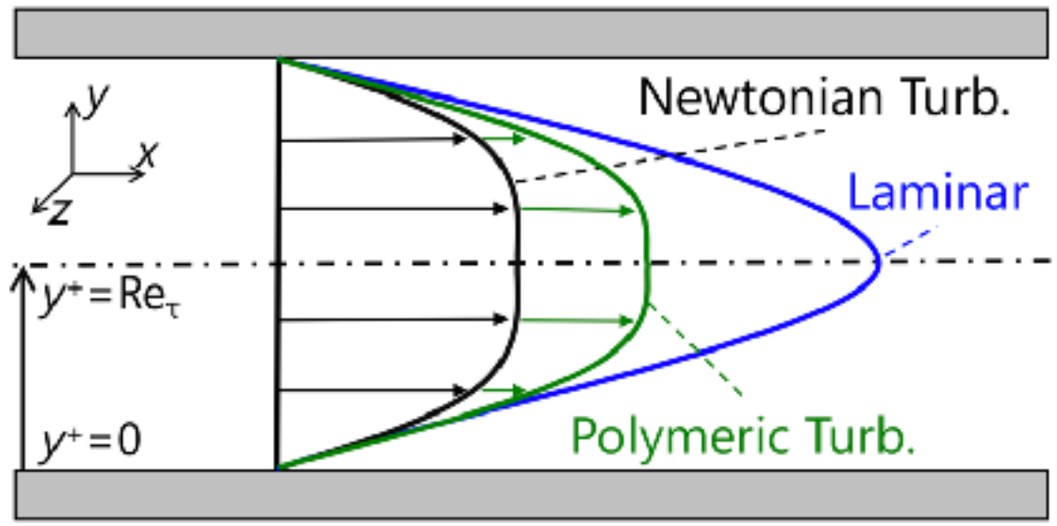

FIG. 1. Drag reduction in turbulent channel flow under a constant pressure gradient (thus, the same wall shear stress).

M. D. Warholic, H. Massah, and T. J. Hanratty, “Influence of drag-reducing polymers on turbulence: Effects of Reynolds number, concentration and mixing,” Exp. Fluids 27, 461–472 (1999)

Polymer Drag Reduction

Toms, B. A. “Some observations on the flow of linear polymer solutions through straight tubes at large Reynolds number,” Proc First Int Congr on Rheol II:135– 141 (1948)

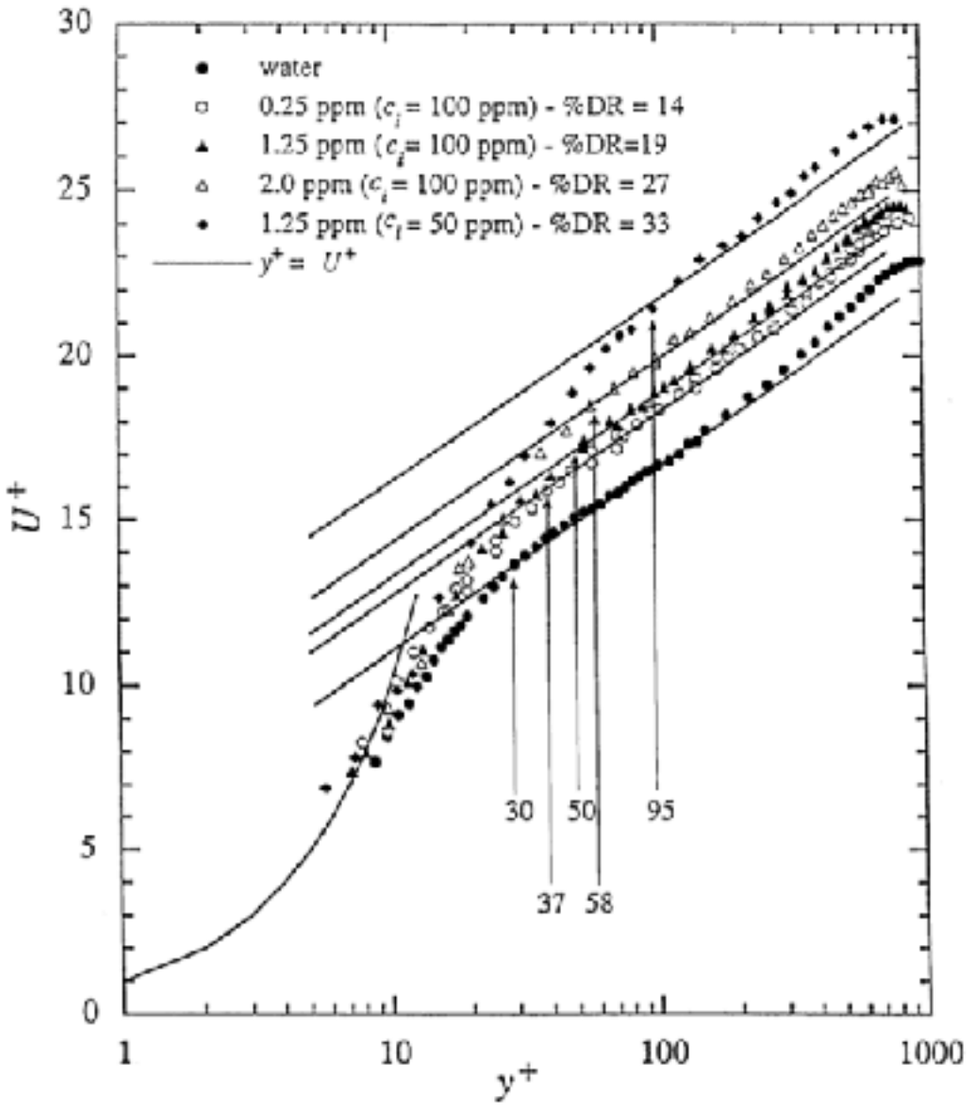

Fig. 3. Non-dimensional streamwise velocity, U^+, versus the non-dimensional distance from the wall, y^+ for low per cent drag reduction runs with best *log layer* fit

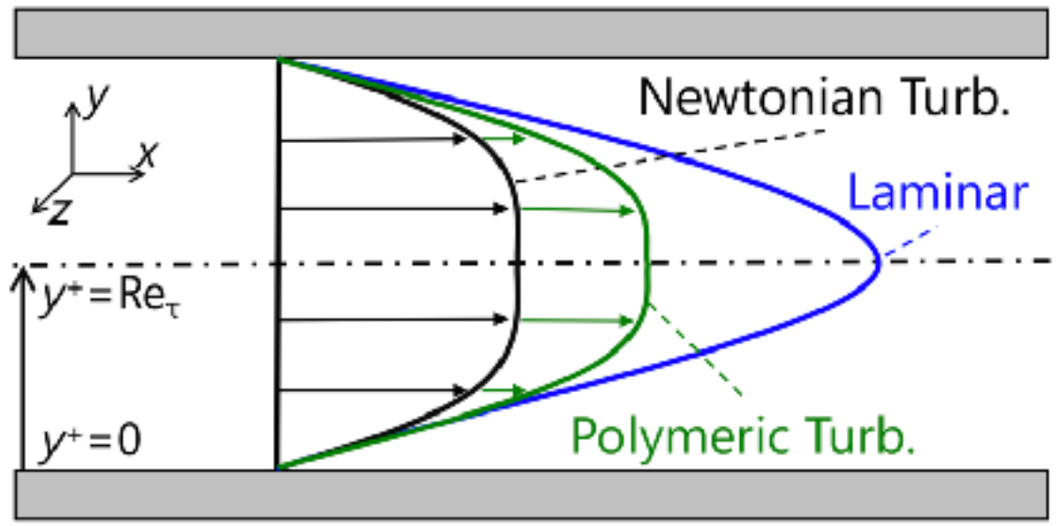

FIG. 1. Drag reduction in turbulent channel flow under a constant pressure gradient (thus, the same wall shear stress).

Polymers additives reduce drag only for turbulent flows, not laminar flows!

M. D. Warholic, H. Massah, and T. J. Hanratty, “Influence of drag-reducing polymers on turbulence: Effects of Reynolds number, concentration and mixing,” Exp. Fluids 27, 461–472 (1999)

Transition to Dissipation in a Model of Superflow

T. Frisch,[1] Y. Pomeau,[2] and S. Rica[1]

[1]*Institut Non Lineaire de Nice, Université de Nice Sophia-Antipolis, Parc Valrose, 06034 Nice CEDEX, France*
[2]*LPS, Ecole Normale Superieure, 24 Rue Lhomond, 75231 Paris CEDEX 05, France*

(Received 29 October 1991; revised manuscript received 2 April 1992)

A direct numerical study of a model of superflow, the nonlinear Schrödinger equation, and simple analytical arguments shows a very striking phenomenon: The flow around a disk creates a drag force beyond a well-defined threshold velocity, linked to the emission of vortices from the perimeter of the disk.

$$i\frac{\partial\Psi}{\partial t}=\frac{1}{2}\Delta\Psi-|\Psi|^2\Psi$$

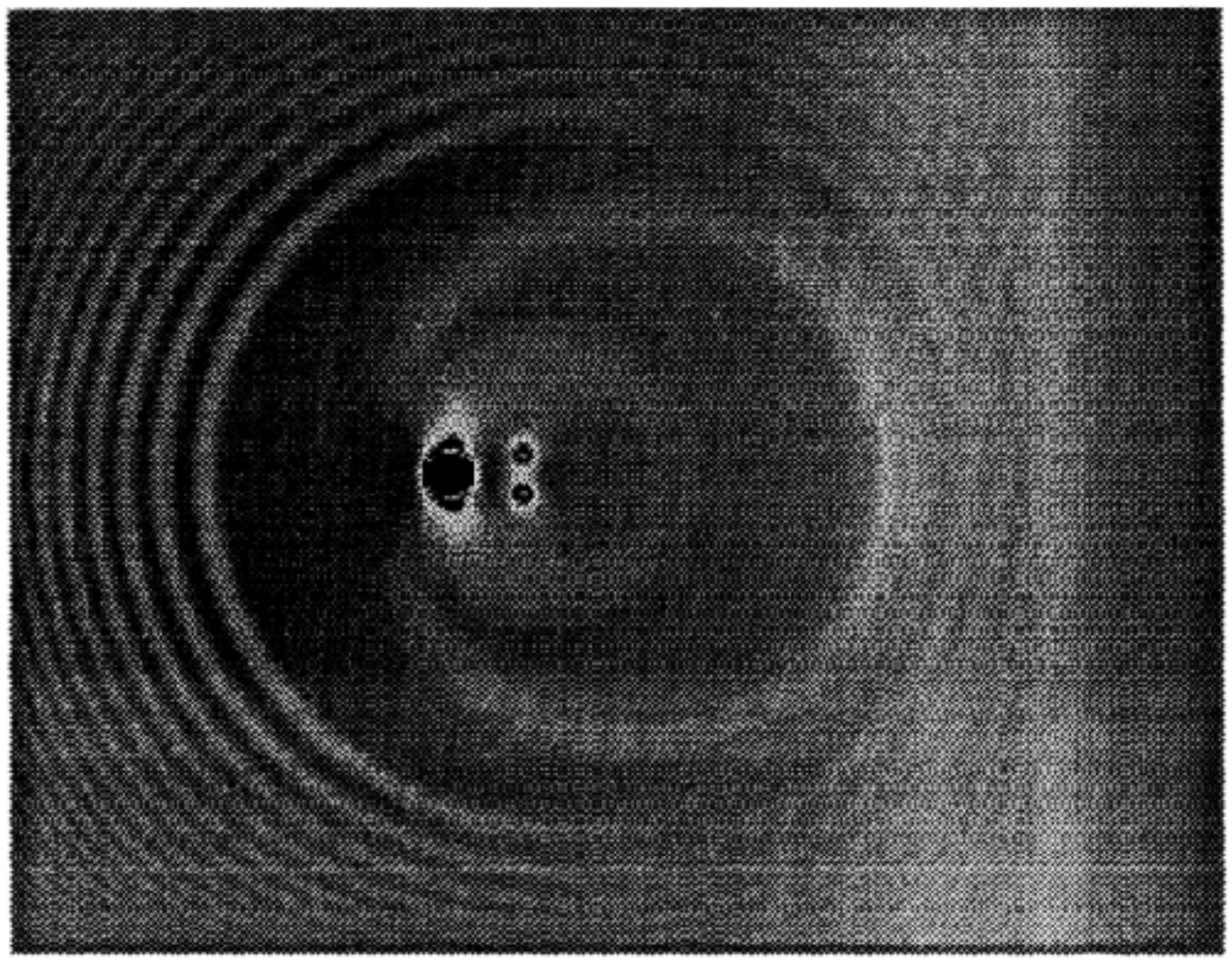

FIG. 1. Cylinder immersed in the "fluid." One represents the modulus of Ψ at an instant of time. The cylinder is the black circle in the middle, and the boundary condition on its surface is $\Psi=0$. The speed at infinity is half the speed of sound, slightly above the onset of drag. This shows that the drag is due to the emission of vortices on the surface of the cylinder at the point of maximal fluid velocity. The vortices appear as white dots close to the cylinder and are convected by the mean flow. The sound waves seen far from the cylinder are transients, not relevant for the onset of continuous drag.

The Josephson-Anderson Relation in Superfluids

Philip W. Anderson
(1923-2020)

In an isothermal, assumed incompressible bath of liquid helium, with free surface at height h in a gravitational field g,

$$\mu = m(p/\rho) + mgh + \tfrac{1}{2}mv_s^2.$$

$$\langle \mu_1 - \mu_2 \rangle_{Av} = h \langle dn/dt \rangle_{Av},$$

where $\langle dn/dt \rangle_{Av}$ is the average rate of motion of vortices across a path from 1 to 2. This is the "phase slippage"

Considerations on the Flow of Superfluid Helium, Reviews of Modern Physics, vol.38, no.2, 298-310 (1966)

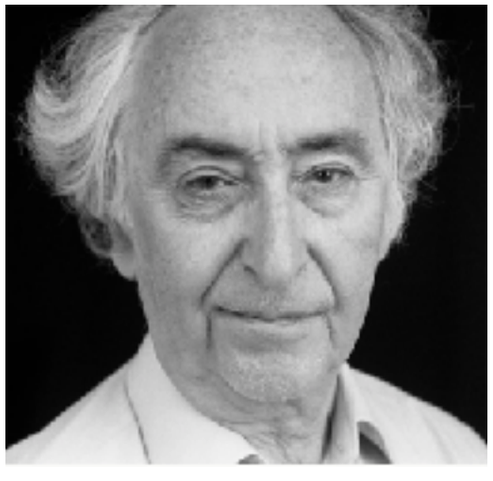

Brian D. Josephson
(1940-present)

The difference between the chemical potentials at two points in a superconductor is equal to (1/c) times the rate at which flux crosses a curve joining the two points inside the superconductor.

Potential Differences in the Mixed State of Type II Superconductors Phys. Lett. vol.16, no. 3, 242-243 (1965)

Resistance in High-Temperature Superconductors

Researchers are beginning to see how the motion of magnetic vortices in these materials can interfere with the flow of current

by David J. Bishop, Peter L. Gammel and David A. Huse

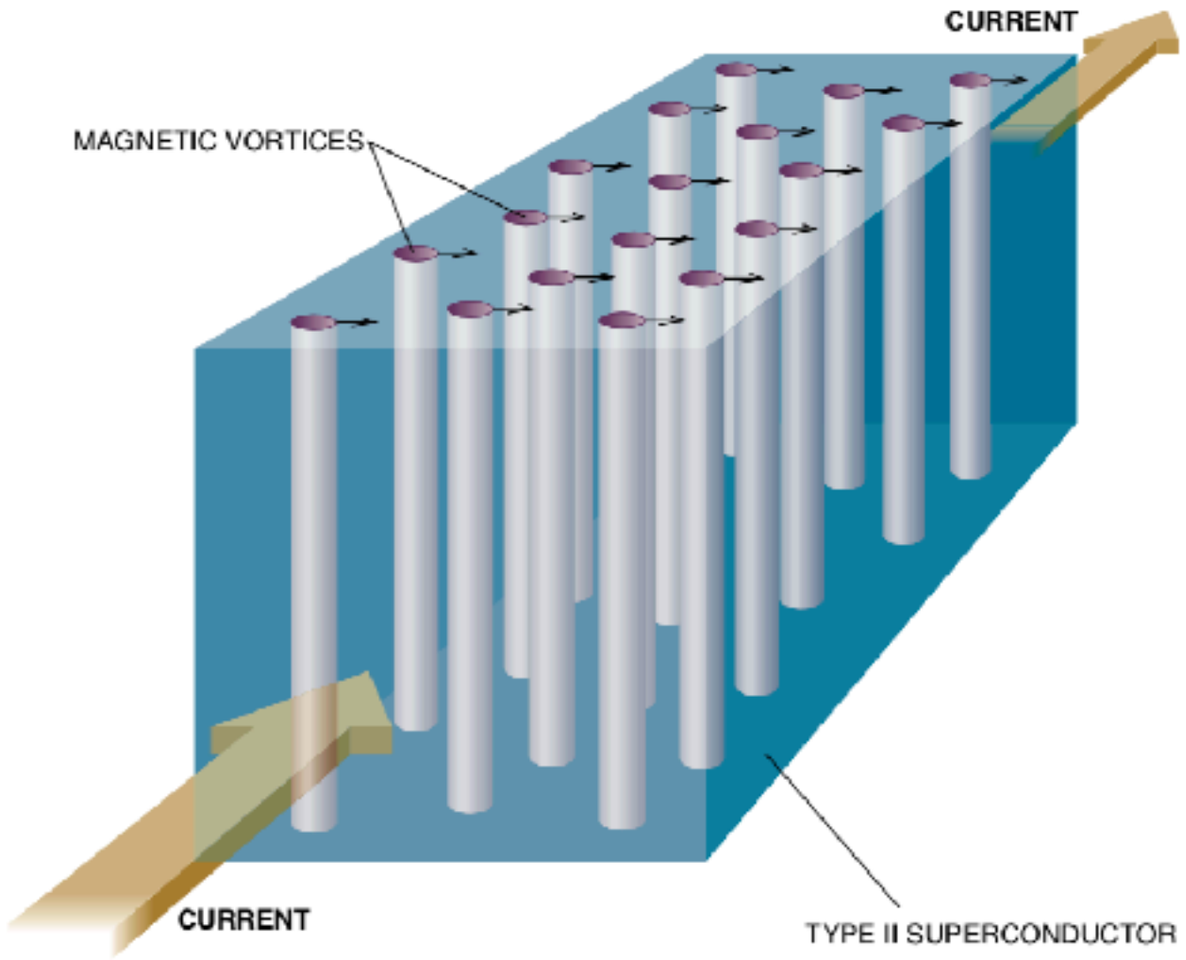

CURRENT FLOW through a superconductor (*blue rectangular box*) can be disrupted by vortices (*cylinders*). Each vortex consists of a ring of circulating current induced by an external magnetic field (*not shown*). The applied current adds to the circulating current on one side of the vortex but subtracts from the other. The net result is a force that pushes the vortices at right angles to the current flow; the movement dissipates energy and produces resistance.

Josephson-Anderson Relation in Classical Fluids?

Philip W. Anderson
(1923-2020)

APPENDIX B. A "NEW" COROLLARY IN CLASSICAL HYDRODYNAMICS?

corollary of Euler's equation:

$$\langle (\tfrac{1}{2}v^2+\mu)_{P_2} \rangle_{\text{Av}} - \langle (\tfrac{1}{2}v^2+\mu)_{P_1} \rangle_{\text{Av}} = \left\langle 2\int_{P_1}^{P_2} d\mathbf{l}\cdot(v\times\omega) \right\rangle_{\text{Av}}$$

one can only assume that it was understood by the "classics" but is of no value in classical hydrodynamics so was never stated.

Considerations on the Flow of Superfluid Helium, Reviews of Modern Physics, vol.38, no.2, 298-310 (1966)

"This result is of no special importance in classical hydrodynamics because the velocity circulation carried by each vortex, albeit constant, can take any value, while in the superfluid it is directly related to the phase of the macroscopic wave function and quantized." — E. Varoquaux, Rev. Mod. Phys. (2015)

Taylor, G. I. The transport of vorticity and heat through fluids in turbulent motion. Proc. Roy. Soc. Lond. A, 135: 685–702 (1932)

In order to express the idea that vorticity rather than momentum is conveyed from one level to another by means of eddies

$$-\frac{1}{\rho}\frac{d\overline{p}}{dx} = 2\overline{w\eta}$$

writing $\eta = \frac{1}{2}\left(\frac{\partial u}{\partial z} - \frac{\partial w}{\partial x}\right)$

Lighthill, M. J. 1963 Boundary layer theory. In Laminar Boundary Layers (ed. L. Rosenhead), pp. 46–113. Oxford University Press, Oxford.

M. James Lighthill
(1924-1998)

The tangential-vorticity source strength has a simple relation to pressure gradient, at least for flow over a stationary plane surface. If the surface is taken as $z = 0$, the flow of x-vorticity out of it is

$$-\nu\frac{\partial\omega_x}{\partial z} = -\nu\frac{\partial}{\partial z}\left(\frac{\partial v_z}{\partial y} - \frac{\partial v_y}{\partial z}\right) = \nu\frac{\partial^2 v_y}{\partial z^2} = \nu\nabla^2 v_y = \frac{1}{\rho}\frac{\partial p}{\partial y}, \qquad (3)$$

since v_x, v_y, v_z are zero on $z = 0$ (whence all their derivatives with respect to x and y vanish, and hence also $\partial v_z/\partial z = 0$ by the solenoidality condition), and because at a solid surface transfer of momentum by convection is absent, so that transfer by diffusion must exactly balance transfer by pressure gradient.

It follows from (3) that the tangential vorticity created is in the direction of the surface isobars (the sense of rotation being that of a ball rolling down the line of steepest pressure fall), and that the source strength per unit area is of magnitude ρ^{-1} times the pressure gradient.

Taylor, G. I. The transport of vorticity and heat through fluids in turbulent motion. Proc. Roy. Soc. Lond. A, 135: 685–702 (1932)

In order to express the idea that vorticity rather than momentum is conveyed from one level to another by means of eddies

$$-\frac{1}{\rho}\frac{d\overline{p}}{dx} = 2\overline{w\eta}$$

writing $\eta = \frac{1}{2}\left(\frac{\partial u}{\partial z} - \frac{\partial w}{\partial x}\right)$

Lighthill, M. J. 1963 Boundary layer theory. In Laminar Boundary Layers (ed. L. Rosenhead), pp. 46–113. Oxford University Press, Oxford.

M. James Lighthill
(1924-1998)

The tangential-vorticity source strength has a simple relation to pressure gradient, at least for flow over a stationary plane surface. If the surface is taken as $z = 0$, the flow of x-vorticity out of it is

$$-\nu\frac{\partial\omega_x}{\partial z} = -\nu\frac{\partial}{\partial z}\left(\frac{\partial v_z}{\partial y} - \frac{\partial v_y}{\partial z}\right) = \nu\frac{\partial^2 v_y}{\partial z^2} = \nu\nabla^2 v_y = \frac{1}{\rho}\frac{\partial p}{\partial y}, \qquad (3)$$

since v_x, v_y, v_z are zero on $z = 0$ (whence all their derivatives with respect to x and y vanish, and hence also $\partial v_z/\partial z = 0$ by the solenoidality condition), and because at a solid surface transfer of momentum by convection is absent, so that transfer by diffusion must exactly balance transfer by pressure gradient.

It follows from (3) that the tangential vorticity created is in the direction of the surface isobars (the sense of rotation being that of a ball rolling down the line of steepest pressure fall), and that the source strength per unit area is of magnitude ρ^{-1} times the pressure gradient.

PHYSICAL REVIEW A VOLUME 1, NUMBER 2 FEBRUARY 1970

Energy-Dissipation Theorem and Detailed Josephson Equation for Ideal Incompressible Fluids

Elisha R. Huggins
Department of Physics and Astronomy, Dartmouth College, Hanover, New Hampshire* 03755†

and

Los Alamos Scientific Laboratory, University of California, Los Alamos, New Mexico 87544
(Received 14 August 1969)

The dissipation of energy in the flow of an ideal incompressible fluid is described by a theorem whose derivation relies upon the exact three-dimensional Magnus formula discussed in the previous paper. The theorem, which explicitly demonstrates the role of vortex motion in the process of energy dissipation, can be used to calculate the trajectories of vortices. Also derived is a detailed Josephson equation – an extension of Anderson's "new corollary in classical hydrodynamics" – which provides an exact non-time-average relation between chemical potentials and vortex motion.

Elisha R. Huggins
(1934-2019)

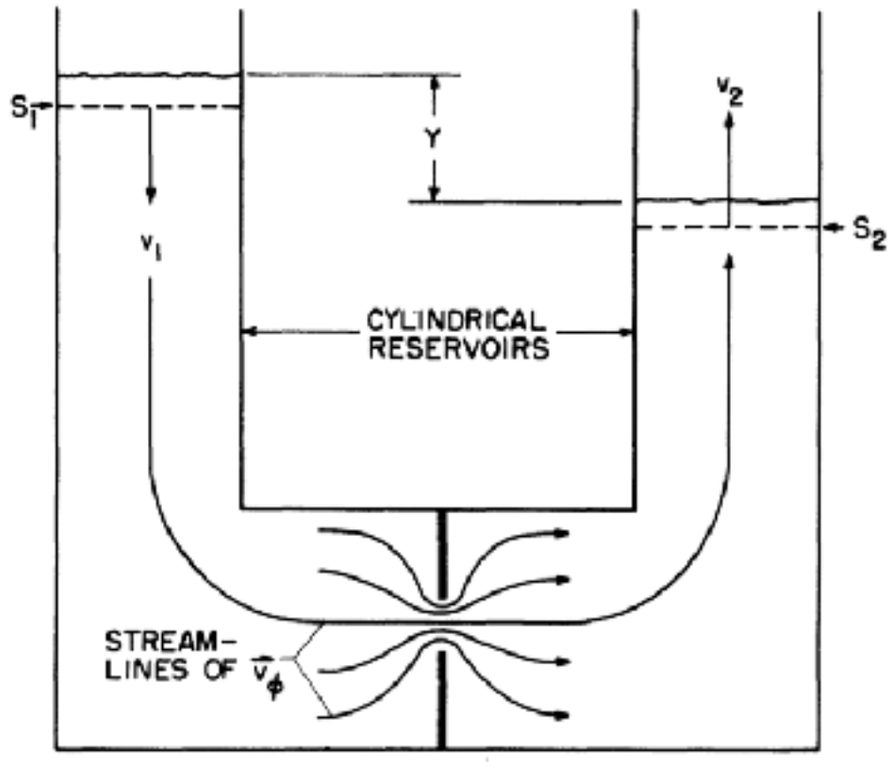

PHYSICAL REVIEW A VOLUME 1, NUMBER 2 FEBRUARY 1970

Energy-Dissipation Theorem and Detailed Josephson Equation for Ideal Incompressible Fluids

Elisha R. Huggins
Department of Physics and Astronomy, Dartmouth College, Hanover, New Hampshire* 03755†

and

Los Alamos Scientific Laboratory, University of California, Los Alamos, New Mexico 87544
(Received 14 August 1969)

The dissipation of energy in the flow of an ideal incompressible fluid is described by a theorem whose derivation relies upon the exact three-dimensional Magnus formula discussed in the previous paper. The theorem, which explicitly demonstrates the role of vortex motion in the process of energy dissipation, can be used to calculate the trajectories of vortices. Also derived is a detailed Josephson equation – an extension of Anderson's "new corollary in classical hydrodynamics" – which provides an exact non-time-average relation between chemical potentials and vortex motion.

Elisha R. Huggins
(1934-2019)

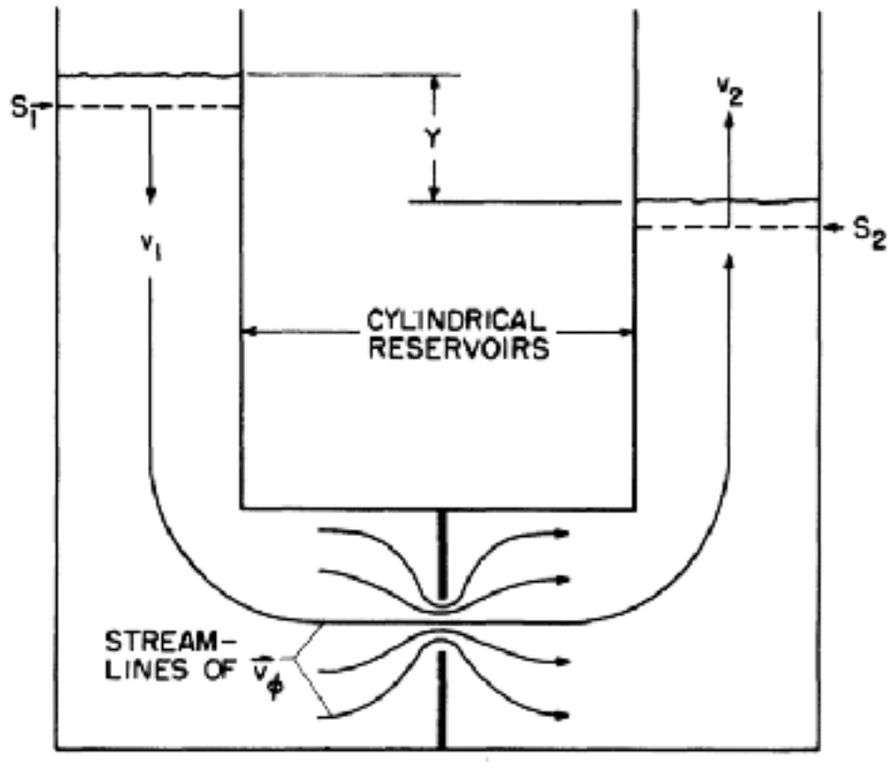

Huggins Vorticity Current Tensor

Huggins (1970,1971) starts with the incompressible Navier-Stokes equation, including an external potential U (e.g. gravity) and a non-potential force $\mathbf{g}$ (e.g. polymer stress):

$$\partial_t \mathbf{u} = \mathbf{u} \times \boldsymbol{\omega} - \nu \nabla \times \boldsymbol{\omega} - \mathbf{g} - \nabla \left(p + U + \frac{1}{2} |\mathbf{u}|^2 \right).$$

Huggins rewrote this as

$$\partial_t u_i = \frac{1}{2} \epsilon_{ijk} \Sigma_{jk} - \partial_i h$$

where $h = p + U + \frac{1}{2} |\mathbf{u}|^2$ is total pressure (hydrostatic + dynamic) and

$$\Sigma_{ij} = u_i \omega_j - u_j \omega_i + \nu \left(\frac{\partial \omega_i}{\partial x_j} - \frac{\partial \omega_j}{\partial x_i} \right) - \epsilon_{ijk} g_k$$

is an anti-symmetric vorticity current tensor which represents flux of j-component of vorticity in the coordinate i-direction $\partial_t \omega_j + \partial_i \Sigma_{ij} = 0$. It is related to Lighthill's "vorticity source vector" $\boldsymbol{\sigma}$ by

$$\boldsymbol{\sigma} = \hat{\mathbf{n}} \cdot \boldsymbol{\Sigma} = \hat{\mathbf{n}} \times \nu (\nabla \times \boldsymbol{\omega}) + \hat{\mathbf{n}} \times \mathbf{g} = - \hat{\mathbf{n}} \times (\nabla h + \partial_t \mathbf{u})$$

which it extends into the flow interior. A mean gradient in h implies mean vorticity flux:

$$\langle \Sigma_{ij} \rangle = \epsilon_{ijk} \partial_k \langle h \rangle$$

Huggins Vorticity Current Tensor

Huggins (1970,1971) starts with the incompressible Navier-Stokes equation, including an external potential U (e.g. gravity) and a non-potential force $\mathbf{g}$ (e.g. polymer stress):

$$\partial_t \mathbf{u} = \mathbf{u} \times \boldsymbol{\omega} - \nu \nabla \times \boldsymbol{\omega} - \mathbf{g} - \nabla \left(p + U + \frac{1}{2} |\mathbf{u}|^2 \right).$$

Huggins rewrote this as

$$\partial_t u_i = \frac{1}{2} \epsilon_{ijk} \Sigma_{jk} - \partial_i h$$

where $h = p + U + \frac{1}{2} |\mathbf{u}|^2$ is total pressure (hydrostatic + dynamic) and

$$\Sigma_{ij} = u_i \omega_j - u_j \omega_i + \nu \left(\frac{\partial \omega_i}{\partial x_j} - \frac{\partial \omega_j}{\partial x_i} \right) - \epsilon_{ijk} g_k$$

is an anti-symmetric vorticity current tensor which represents flux of j-component of vorticity in the coordinate i-direction $\partial_t \omega_j + \partial_i \Sigma_{ij} = 0$. It is related to Lighthill's "vorticity source vector" $\boldsymbol{\sigma}$ by

$$\boldsymbol{\sigma} = \hat{\mathbf{n}} \cdot \boldsymbol{\Sigma} = \hat{\mathbf{n}} \times \nu (\nabla \times \boldsymbol{\omega}) + \hat{\mathbf{n}} \times \mathbf{g} = - \hat{\mathbf{n}} \times (\nabla h + \partial_t \mathbf{u})$$

which it extends into the flow interior. A mean gradient in h implies mean vorticity flux:

$$\langle \Sigma_{ij} \rangle = \epsilon_{ijk} \partial_k \langle h \rangle$$

Huggins Vorticity Current Tensor

Huggins (1970,1971) starts with the incompressible Navier-Stokes equation, including an external potential U (e.g. gravity) and a non-potential force $\mathbf{g}$ (e.g. polymer stress):

$$\partial_t \mathbf{u} = \mathbf{u} \times \boldsymbol{\omega} - \nu \nabla \times \boldsymbol{\omega} - \mathbf{g} - \nabla \left(p + U + \frac{1}{2} |\mathbf{u}|^2 \right).$$

Huggins rewrote this as

$$\partial_t u_i = \frac{1}{2} \epsilon_{ijk} \Sigma_{jk} - \partial_i h$$

where $h = p + U + \frac{1}{2} |\mathbf{u}|^2$ is total pressure (hydrostatic + dynamic) and

$$\Sigma_{ij} = u_i \omega_j - u_j \omega_i + \nu \left(\frac{\partial \omega_i}{\partial x_j} - \frac{\partial \omega_j}{\partial x_i} \right) - \epsilon_{ijk} g_k$$

is an anti-symmetric vorticity current tensor which represents flux of j-component of vorticity in the coordinate i-direction $\partial_t \omega_j + \partial_i \Sigma_{ij} = 0$. It is related to Lighthill's "vorticity source vector" $\boldsymbol{\sigma}$ by

$$\boldsymbol{\sigma} = \hat{\mathbf{n}} \cdot \boldsymbol{\Sigma} = \hat{\mathbf{n}} \times \nu (\nabla \times \boldsymbol{\omega}) + \hat{\mathbf{n}} \times \mathbf{g} = - \hat{\mathbf{n}} \times (\nabla h + \partial_t \mathbf{u})$$

which it extends into the flow interior. A mean gradient in h implies mean vorticity flux:

$$\langle \Sigma_{ij} \rangle = \epsilon_{ijk} \partial_k \langle h \rangle$$

Flow Past a Finite Solid Body

PHYSICAL REVIEW X **11,** 031054 (2021)

Featured in Physics

Josephson-Anderson Relation and the Classical D'Alembert Paradox

Gregory L. Eyink[1,2]

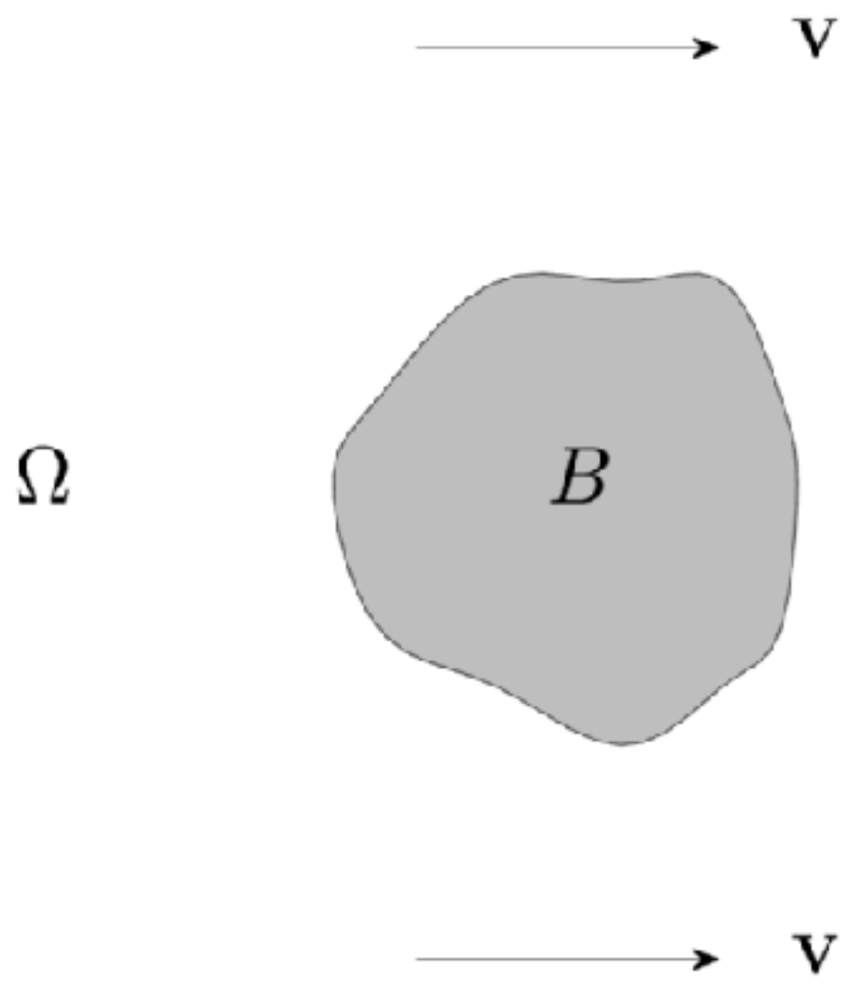

FIG. 2 Flow around a finite body B in an unbounded region Ω filled with fluid moving at a velocity $\mathbf{V}$ at far distances.

Ideal Euler Flow Past a Solid Body

The potential solution of the incompressible Euler equation for flow past body B

$$\partial_t \mathbf{u}_\phi + \boldsymbol{\nabla}\cdot(\mathbf{u}_\phi \mathbf{u}_\phi + p_\phi \mathbf{I}) = \mathbf{0}, \quad \boldsymbol{\nabla}\cdot\mathbf{u}_\phi = 0$$

can be solved for the velocity potential ϕ in $\mathbf{u}_\phi = \boldsymbol{\nabla}\phi$ from the Laplace problem

$$\triangle\phi = 0 \qquad \left.\frac{\partial\phi}{\partial n}\right|_{\partial B} = 0, \quad \phi \underset{|\mathbf{x}|\to\infty}{\sim} \mathrm{V}x$$

with kinematic pressure p_ϕ given by the Bernoulli equation

$$\partial_t\phi + \frac{1}{2}|\mathbf{u}_\phi|^2 + p_\phi = const.$$

The force that the fluid exerts on the body arises from pressure $P_\phi = \rho p_\phi$

$$\mathbf{F}_\phi = -\int_{\partial B} P_\phi\, \hat{\mathbf{n}}\, dA$$

and by d'Alembert's result has vanishing drag component, $\mathbf{V}\cdot\mathbf{F}_\phi = 0$. Finally, define $\mathbf{u}_\omega = \mathbf{u} - \mathbf{u}_\phi$ as the complementary velocity field of the rotational motions.

The Detailed Josephson-Anderson Relation for Flow Past a Body

For the incompressible Navier-Stokes solution, the reaction force of the body back on the fluid

$$\mathbf{F} = \int_{\partial B} (P_\omega \hat{\mathbf{n}} - 2\eta\, \mathbf{S}\, \hat{\mathbf{n}}) dA$$

is given *instantaneously* by

$$\begin{aligned} -\mathbf{F}\cdot\mathbf{V} &= -\rho \int_\Omega \mathbf{u}_\phi \cdot (\mathbf{u}\times\boldsymbol{\omega} - \nu\nabla\times\boldsymbol{\omega} - \mathbf{g})\, dV \\ &= -\int dJ \int (\mathbf{u}\times\boldsymbol{\omega} - \nu\nabla\times\boldsymbol{\omega} - \mathbf{g})\cdot d\boldsymbol{\ell} \\ &= -\frac{1}{2}\int dJ \int \epsilon_{ijk}\Sigma_{ij} d\ell_k, \end{aligned}$$

"The equation provides an elegant short cut to certain predictions that involve the complex motion of quantized vortices. These same predictions by other methods require a detailed knowledge of vortex motion and involve considerable computational effort." — R. E. Packard, "The role of the Josephson-Anderson equation in superfluid helium," Rev. Mod. Phys. 70: 641 (1998)

The Detailed Josephson-Anderson Relation for Flow Past a Body

For the incompressible Navier-Stokes solution, the reaction force of the body back on the fluid

$$\mathbf{F} = \int_{\partial B} (P_\omega \hat{\mathbf{n}} - 2\eta\, \mathbf{S}\, \hat{\mathbf{n}}) dA$$

is given *instantaneously* by

$$\begin{aligned} -\mathbf{F}\cdot\mathbf{V} &= -\rho \int_\Omega \mathbf{u}_\phi \cdot (\mathbf{u}\times\boldsymbol{\omega} - \nu\nabla\times\boldsymbol{\omega} - \mathbf{g})\, dV \\ &= -\int dJ \int (\mathbf{u}\times\boldsymbol{\omega} - \nu\nabla\times\boldsymbol{\omega} - \mathbf{g})\cdot d\boldsymbol{\ell} \\ &= -\frac{1}{2}\int dJ \int \epsilon_{ijk}\Sigma_{ij} d\ell_k, \end{aligned}$$

First interpretation: Drag occurs when the vortex force $\mathbf{f}_v = \mathbf{u}\times\boldsymbol{\omega} - \nu\nabla\times\boldsymbol{\omega} - \mathbf{g}$ acts against the background potential flow velocity $\mathbf{u}_\phi$:

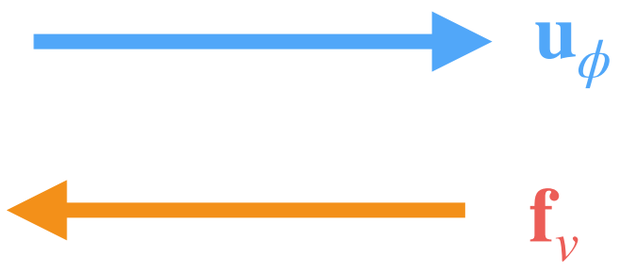

The Detailed Josephson-Anderson Relation for Flow Past a Body

For the incompressible Navier-Stokes solution, the reaction force of the body back on the fluid

$$\mathbf{F} = \int_{\partial B} (P_\omega \hat{\mathbf{n}} - 2\eta\, \mathbf{S}\, \hat{\mathbf{n}}) dA$$

is given *instantaneously* by

$$\begin{aligned} -\mathbf{F}\cdot\mathbf{V} &= -\rho \int_\Omega \mathbf{u}_\phi \cdot (\mathbf{u}\times\boldsymbol{\omega} - \nu\nabla\times\boldsymbol{\omega} - \mathbf{g})\, dV \\ &= -\int dJ \int (\mathbf{u}\times\boldsymbol{\omega} - \nu\nabla\times\boldsymbol{\omega} - \mathbf{g})\cdot d\boldsymbol{\ell} \\ &= -\frac{1}{2}\int dJ \int \epsilon_{ijk}\Sigma_{ij} d\ell_k, \end{aligned}$$

Second interpretation: Drag occurs when a <u>transverse/spanwise vorticity</u> component ω_z experiences flux Σ_{yz} in the orthogonal y-direction across potential flow-lines:

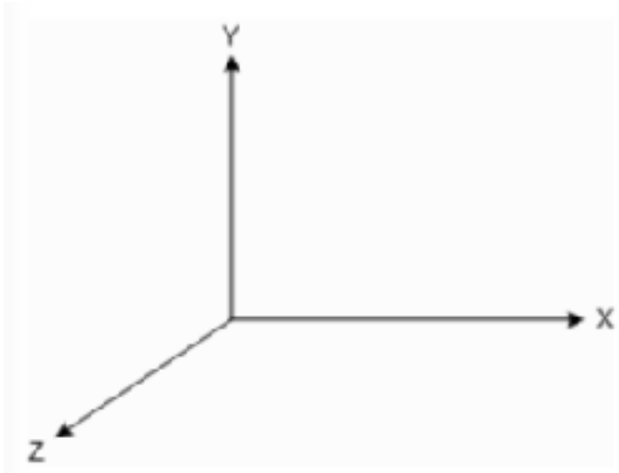

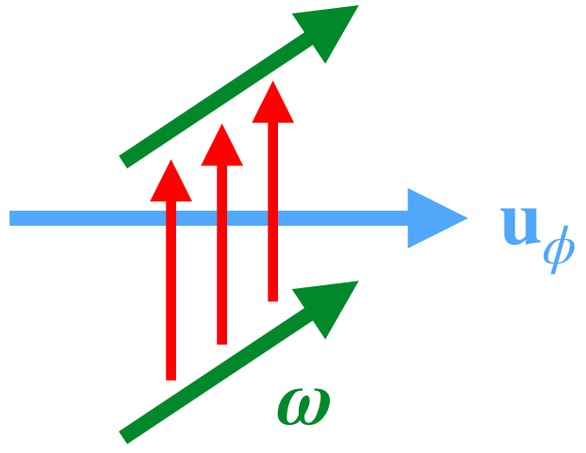

Drag Creation by Outward Flux of Vorticity

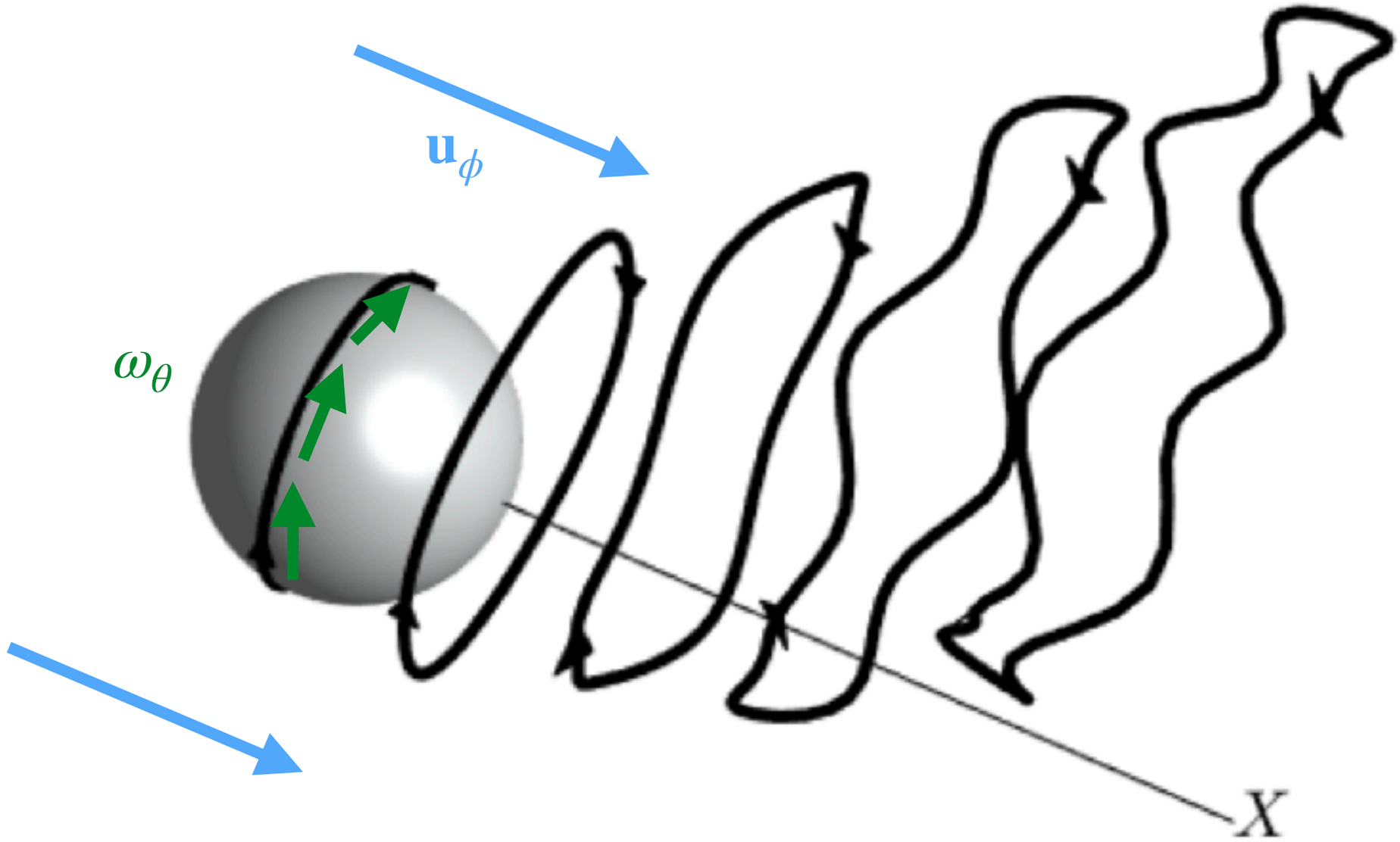

Negative azimuthal vorticity $\omega_\theta < 0$ is
created by pressure-drop around the sphere

Drag Creation by Outward Flux of Vorticity

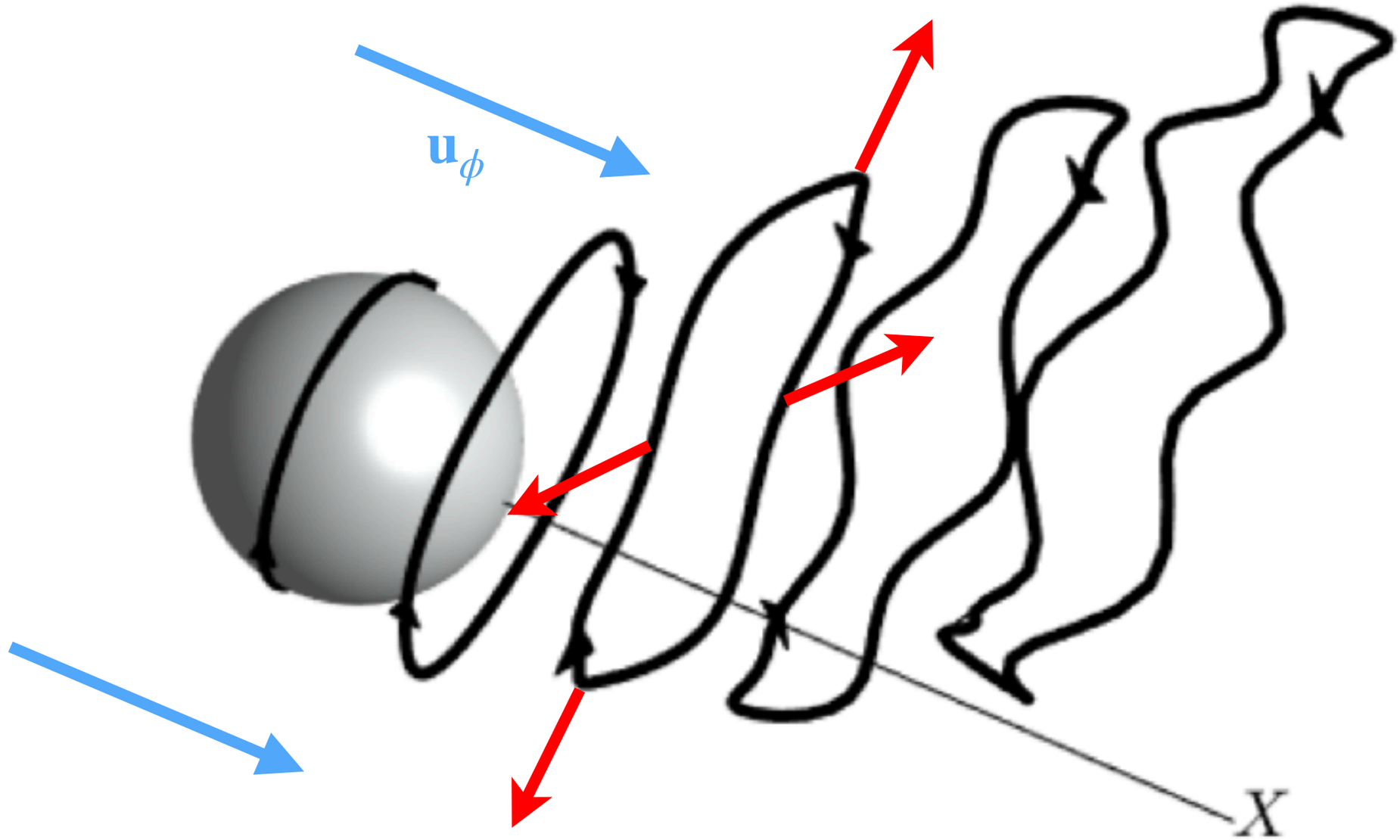

Vortex loops expand radially outward, subtending more mass flux J and subtracting energy from the potential flow and transferring it to rotational motions in the wake.

JA-Relation in Work Form

The energy transfer $\mathscr{T}$ in the JA-relation can be rewritten using integration by parts as

$$\begin{aligned}\mathscr{T} &= -\rho \int_{\Omega} \mathbf{u}_{\phi} \cdot (\mathbf{u} \times \boldsymbol{\omega} - \nu \nabla \times \boldsymbol{\omega} - \mathbf{g})\, dV \\ &= -\rho \int_{\Omega} \nabla \mathbf{u}_{\phi} : (\mathbf{u}_{\omega}\mathbf{u}_{\omega} + \boldsymbol{\tau}_{g})\, dV + \int_{\partial\Omega} \mathbf{u}_{\phi} \cdot \boldsymbol{\tau}_{w}\, dA\end{aligned}$$

assuming furthermore that the body-force $\mathbf{g} = \nabla \cdot \boldsymbol{\tau}_{g}$ in terms of a corresponding stress-tensor $\boldsymbol{\tau}_{g}$ (e.g. the stress of a polymer additive).

The term $-\rho \nabla \mathbf{u}_{\phi} : (\mathbf{u}_{\omega}\mathbf{u}_{\omega} + \boldsymbol{\tau}_{g})$ represents deformation work by the total stress of rotational motions and body stress acting against the potential strain field.
stress-tensor $\boldsymbol{\tau}_{g}$ (e.g. the stress of a polymer additive).

With skin friction $\boldsymbol{\tau}_{w} = 2\eta \mathbf{S} \cdot \hat{\mathbf{n}} = \eta \boldsymbol{\omega} \times \hat{\mathbf{n}} = \eta(\partial \mathbf{u}/\partial n)$, the final term $\mathbf{u}_{\phi} \cdot \boldsymbol{\tau}_{w}$ represents work of surface viscous force against the surface potential flow.

JA-Relation in Work Form

The energy transfer $\mathscr{T}$ in the JA-relation can be rewritten using integration by parts as

$$\mathscr{T} = -\rho \int_{\Omega} \mathbf{u}_{\phi} \cdot (\mathbf{u} \times \boldsymbol{\omega} - \nu \nabla \times \boldsymbol{\omega} - \mathbf{g})\, dV$$

$$= -\rho \int_{\Omega} \nabla \mathbf{u}_{\phi} : (\mathbf{u}_{\omega}\mathbf{u}_{\omega} + \boldsymbol{\tau}_{g})\, dV + \int_{\partial\Omega} \mathbf{u}_{\phi} \cdot \boldsymbol{\tau}_{w}\, dA$$

assuming furthermore that the body-force $\mathbf{g} = \nabla \cdot \boldsymbol{\tau}_{g}$ in terms of a corresponding stress-tensor $\boldsymbol{\tau}_{g}$ (e.g. the stress of a polymer additive).

The term $-\rho \nabla \mathbf{u}_{\phi} : (\mathbf{u}_{\omega}\mathbf{u}_{\omega} + \boldsymbol{\tau}_{g})$ represents deformation work by the total stress of rotational motions and body stress acting against the potential strain field.
stress-tensor $\boldsymbol{\tau}_{g}$ (e.g. the stress of a polymer additive).

With skin friction $\boldsymbol{\tau}_{w} = 2\eta \mathbf{S} \cdot \hat{\mathbf{n}} = \eta \boldsymbol{\omega} \times \hat{\mathbf{n}} = \eta(\partial \mathbf{u}/\partial n)$, the final term $\mathbf{u}_{\phi} \cdot \boldsymbol{\tau}_{w}$ represents work of surface viscous force against the surface potential flow.

JA-Relation in Work Form

The energy transfer $\mathscr{T}$ in the JA-relation can be rewritten using integration by parts as

$$\begin{aligned}\mathscr{T} &= -\rho \int_{\Omega} \mathbf{u}_{\phi} \cdot (\mathbf{u} \times \boldsymbol{\omega} - \nu \nabla \times \boldsymbol{\omega} - \mathbf{g})\, dV \\ &= -\rho \int_{\Omega} \nabla \mathbf{u}_{\phi} : (\mathbf{u}_{\omega}\mathbf{u}_{\omega} + \boldsymbol{\tau}_{g})\, dV + \int_{\partial\Omega} \mathbf{u}_{\phi} \cdot \boldsymbol{\tau}_{w}\, dA\end{aligned}$$

assuming furthermore that the body-force $\mathbf{g} = \nabla \cdot \boldsymbol{\tau}_g$ in terms of a corresponding stress-tensor $\boldsymbol{\tau}_g$ (e.g. the stress of a polymer additive).

The term $-\rho \nabla \mathbf{u}_{\phi} : (\mathbf{u}_{\omega}\mathbf{u}_{\omega} + \boldsymbol{\tau}_{g})$ represents deformation work by the total stress of rotational motions and body stress acting against the potential strain field.
stress-tensor $\boldsymbol{\tau}_g$ (e.g. the stress of a polymer additive).

With skin friction $\boldsymbol{\tau}_w = 2\eta \mathbf{S} \cdot \hat{\mathbf{n}} = \eta \boldsymbol{\omega} \times \hat{\mathbf{n}} = \eta(\partial \mathbf{u}/\partial n)$, the final term $\mathbf{u}_{\phi} \cdot \boldsymbol{\tau}_w$ represents work of surface viscous force against the surface potential flow.

The D'Alembert Paradox

Jean le Rond d'Alembert
(1717-1783)

"It seems to me that the theory [potential flow], developed in all possible rigor, gives, at least in several cases, a strictly vanishing resistance, a singular paradox which I leave to future Geometers to elucidate…"

D'Alembert, submission for the 1749 Prize Problem of the Berlin Academy

In the work form, the JA-relation holds even in the limit $Re \to \infty$:

H. Quan and GE, Inertial Momentum Dissipation for Viscosity Solutions of Euler Equations. I. Flow Around a Smooth Body. https://arxiv.org/abs/2206.05325

H. Quan, G. L. Eyink, "Onsager Theory of Turbulence, the Josephson-Anderson Relation, and the D'Alembert Paradox," https://arxiv.org/abs/2206.05326

JA-Relation at Infinite-Re

The JA-relation in the limit $Re \to \infty$ still holds as $-\mathbf{F} \cdot \mathbf{V} = \mathscr{T}$ with:

$$\mathbf{F} = \int_{\partial B} (P_\omega \hat{\mathbf{n}} - \boldsymbol{\tau}_w) dA$$

and

$$\mathscr{T} = -\rho \int_\Omega \nabla \mathbf{u}_\phi : \mathbf{u}_\omega \mathbf{u}_\omega \, dV + \int_{\partial\Omega} \mathbf{u}_\phi \cdot \boldsymbol{\tau}_w \, dA$$

If the weak Euler solution has $(\mathbf{u}, p)$ **near-wall bounded** and furthermore satisfies the **no-flow-through** condition in the following precise sense:

$$\lim_{\delta \to 0} \int_0^t \left(\text{ess . sup}_{d(\mathbf{x}) \le \delta} |\, \mathbf{n} \cdot \mathbf{u}(x, s) \,| \right)^2 ds = 0,$$

then we can prove rigorously that $\boldsymbol{\tau}_w = \mathbf{0}$. All of the limiting drag then arises from pressure asymmetry or “form drag”.

We can show that Lighthill’s theory of vorticity generation by tangential pressure gradients also still holds at infinite-Re and thus vorticity still flows from the body surface and generates energy dissipation in the wake by the JA-relation.

Experimental Results: Flow Past a Sphere

Achenbach E. Experiments on the flow past spheres at very high Reynolds numbers. Journal of fluid mechanics. 1972 Aug;54(3):565-75.

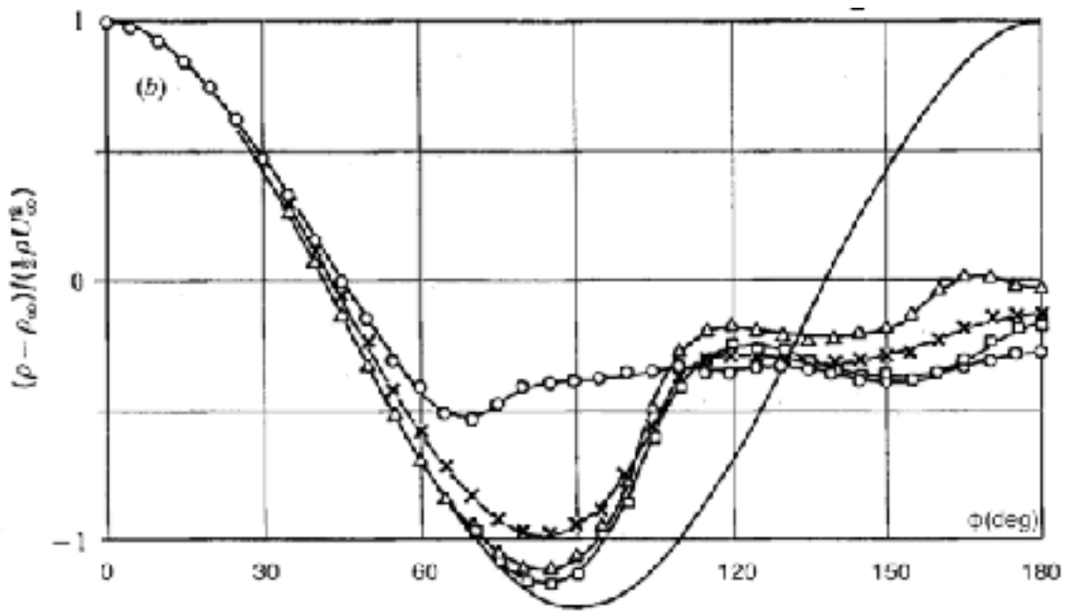

FIGURE 7. (a) Local skin friction and (b) static pressure distribution for the smooth sphere at variable Reynolds numbers. ——, theory. Experiment: —○—, $Re = 1{\cdot}62 \times 10^5$; —×—, $Re = 3{\cdot}18 \times 10^5$; —△—, $Re = 1{\cdot}14 \times 10^5$; —□—, $Re = 5{\cdot}00 \times 10^5$.

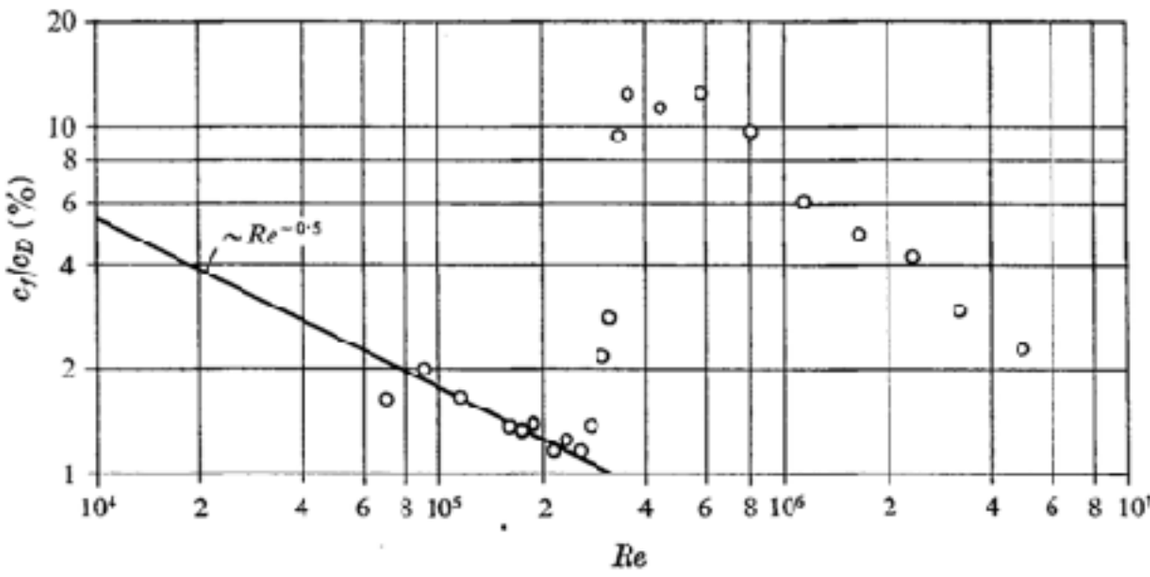

FIGURE 10. Friction forces as a percentage of the total drag for smooth spheres.

These observations suggest that $\boldsymbol{\tau}_w = \mathbf{0}$ for flow past a sphere and that all of the limiting drag arises here from pressure asymmetry, or <u>form drag</u>.

An Experimental Puzzle on Anomalous Dissipation

PHYSICAL REVIEW E VOLUME 56, NUMBER 1 JULY 1997

**Energy injection in closed turbulent flows:
Stirring through boundary layers versus inertial stirring**

O. Cadot,* Y. Couder, A. Daerr, S. Douady, and A. Tsinober†
Laboratoire Physique Statistique, Ecole Normale Supérieure, 24 rue Lhomond, 75231 Paris, France

strong anomaly: flow past a grid, jets through orifices, wakes behind bluff bodies such as cylinders and spheres

weak anomaly: pipe and channel (Poiseuille) flow, developing boundary layer over a flat plate, Taylor-Couette flow, von Kármán flow (or "French washing machine"), Rayleigh-Bénard turbulence…*.except when the walls are rough!*

What is common to all of the flows of the second class is that there is no form drag when the walls are smooth, but form drag appears with wall roughness.

An Experimental Puzzle on Anomalous Dissipation

3-D measurements of the flow around two roughness cubes

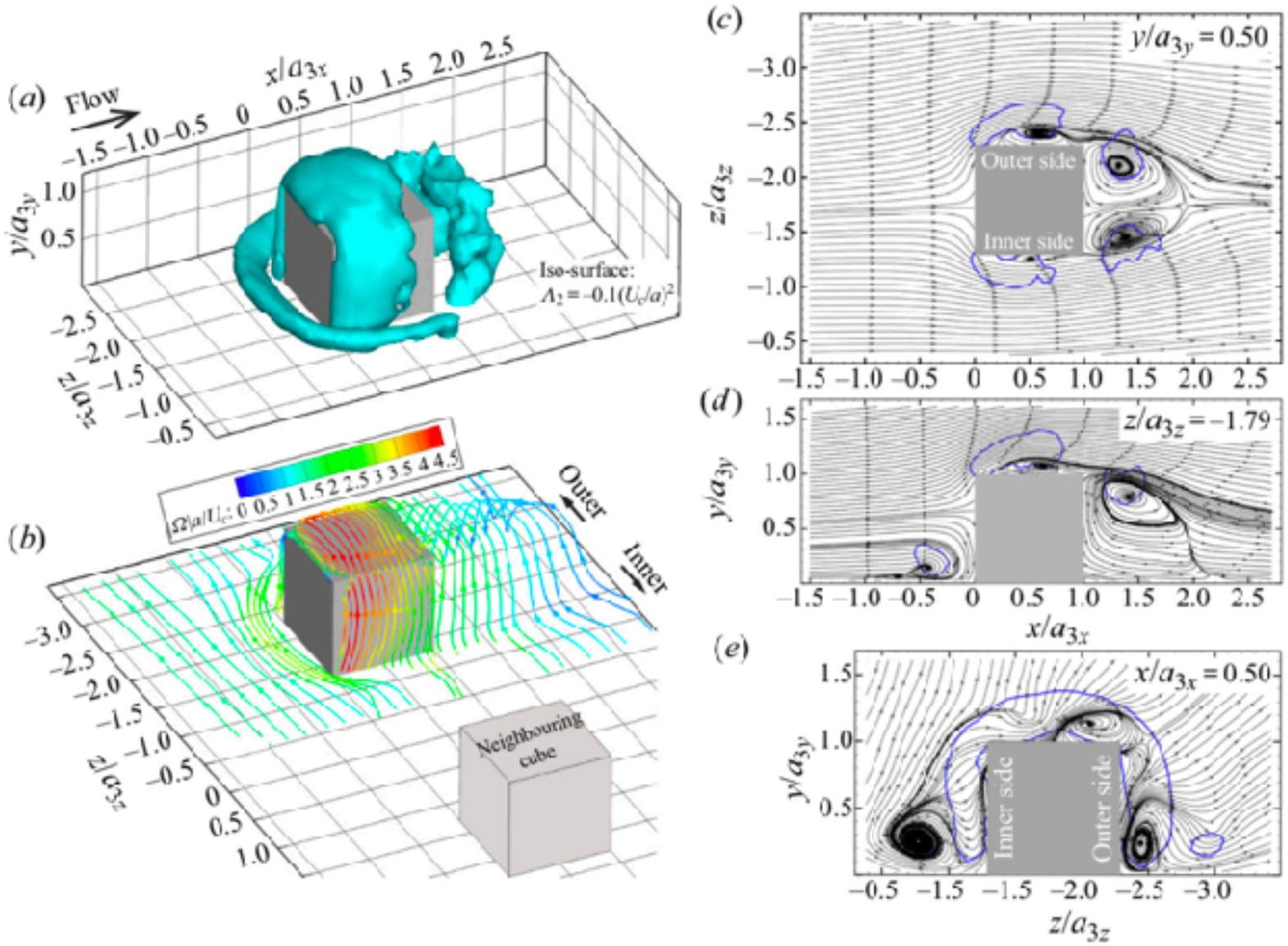

Figure 3. Characteristic primary flow structure around one of the cubes for $\lambda = 2.5a$. (*a*) Iso-surface of $\Lambda_2 = -0.1U_c^2/a^2$; and (*b*) vortex lines colour coded with the vorticity magnitude. (*c–e*) Selected in-plane streamlines: (*c*) *x*–*z* plane at $y/a_{3y} = 0.5$, (*d*) *x*–*y* plane at $z/a_{3z} = -1.79$ and (*e*) *y*–*z* plane at $x/a_{3x} = 0.5$. Blue lines: contour of $\Lambda_2 = -0.1U_c^2/a^2$ showing the intersections with the vortical canopy, arch-like and horseshoe vortices.

J. Gao, K. Agarwal and J. Katz, J. Fluid Mech. (2021), vol. 918, A31, doi:10.1017/jfm.2021.184

An Experimental Puzzle on Anomalous Dissipation

PHYSICAL REVIEW E VOLUME 56, NUMBER 1 JULY 1997

**Energy injection in closed turbulent flows:
Stirring through boundary layers versus inertial stirring**

O. Cadot,* Y. Couder, A. Daerr, S. Douady, and A. Tsinober†
Laboratoire Physique Statistique, Ecole Normale Supérieure, 24 rue Lhomond, 75231 Paris, France

strong anomaly: flow past a grid, jets through orifices, wakes behind bluff bodies such as cylinders and spheres

weak anomaly: pipe and channel (Poiseuille) flow, developing boundary layer over a flat plate, Taylor-Couette flow, von Kármán flow (or “French washing machine”), Rayleigh-Bénard turbulence….except when the walls are rough*!*

What is common to all of the flows of the second class is that there is no form drag when the walls are smooth, but form drag appears with wall roughness.

Form drag described by the JA-relation appears necessary for a strong dissipative anomaly in 3D incompressible fluid turbulence, for laboratory flows.

Wide Generality of the JA-Relation

G. Eyink (in preparation) has shown that the JA-relation holds for any body with arbitrary changes of shape and volume and accelerating in any fashion.

In the rest frame of the body center of mass and with the work form of the transfer term, the relation is:

$$\mathscr{T} = \mathbf{F} \cdot \mathbf{V}(t) + \int_{\partial B(t)} \mathbf{v}_B(t) \cdot d\mathbf{f}, \qquad d\mathbf{f} = \rho \hat{\mathbf{n}} p_\omega \, dA$$

Now $\mathbf{V}(t)$ is instead the velocity of the body (in the fluid frame) while $\mathbf{v}_B(t)$ is the velocity of each surface element (in the body frame), with $d\mathbf{f}$ the pressure force imposed on the fluid by that element.

The JA-relation holds also with Navier-slip boundary conditions, for generalized pipe and channel flows with arbitrarily curved walls, and for spatially periodic boundary conditions that are more convenient for numerical simulations.

Drag Reduction and JA-Relation

Toms, B. A. “Some observations on the flow of linear polymer solutions through straight tubes at large Reynolds number,” Proc First Int Congr on Rheol II:135– 141 (1948)

The JA-relation gives the necessary and sufficient conditions for drag reduction and for drag enhancement! The mean drag is directly related to the mean vorticity flux

$$-\langle \mathbf{F} \rangle \cdot \mathbf{V} = -\frac{1}{2} \int dJ \int \epsilon_{ijk} \langle \Sigma_{ij} \rangle d\ell_k$$

which in turn is related to gradients of total pressure:

$$\langle \Sigma_{ij} \rangle = \epsilon_{ijk} \partial_k \langle h \rangle$$

Drag can be reduced <u>only</u> by reducing the cross-stream flux of spanwise vorticity, and drag can be enhanced <u>only</u> by increasing that flux. <u>This result argues for focused empirical investigation of the vorticity flux in drag-reduced and drag-enhanced flow.</u>

Dataset description

Channel flow:

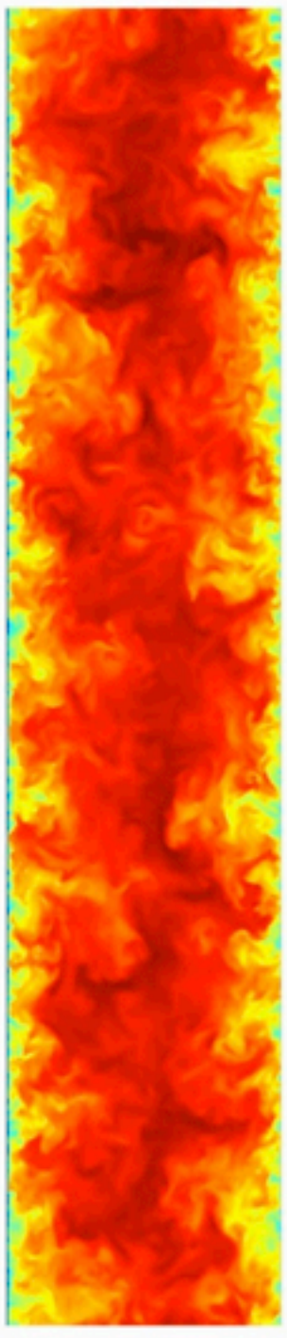

Simulation data provenance: Collaboration of UT Austin and JHU, using the UT Austin DNS code (see README-CHANNEL for more details).

- Direct numerical simulation (DNS) of channel flow in a domain of size 8π x 2 x 3π , using 2048 x 512 x 1536 nodes.
- Incompressible Navier-Stokes equations are solved using the pseudo-spectral (Fourier-Galerkin) method in wall-parallel (x, z) planes, and the 7th-order B-spline collocation method in the wall-normal (y) direction.
- Simulation is run and equilibrated using prescribed bulk velocity=1, then switched to imposed pressure gradient (dP/dx = 0.0025) and further equilibrated.
- After the simulation has reached a (nearly) statistical stationary state, 4,000 frames of data with 3 velocity components and pressure are stored in the database. The frames are stored at every 5 time-steps of the DNS. This corresponds to about one channel flow-through time. Intermediate times can be queried using temporal-interpolation.
- The friction velocity is $u_\tau = 0.0499$.
- The viscosity is $\nu = 5 \times 10^{-5}$.
- The friction velocity Reynolds number is $Re_\tau \sim 1000$.
- The y-locations of the grid points in the vertical direction can be downloaded from this text file; the corresponding B-spline knot locations can be obtained from this text file.
- A table with the time history of friction velocity Reynolds number can be downloaded from this text file.
- A table with the vertical profiles of mean velocity, Reynolds shear stresses, viscous stress, normal stress, mean pressure, pressure variance and pressure-velocity covariance in viscous units, can be downloaded from this text file.
- Files with tables of the streamwise (k_x) spectra of u, v, w, p at various heights can be downloaded for the following y+ values: 10.11, 29.89, 99.75, 371.6, and 999.7.
- Files with tables of the spanwise (k_z) spectra of u, v, w, p at various heights can be downloaded for the following y+ values: 10.11, 29.89, 99.75, 371.6, and 999.7.

The Detailed Josephson-Anderson Relation for Channel-Flow

$$\int dJ\,(h_\omega^{in} - h_\omega^{out}) = -\,\rho \int_\Omega \mathbf{u}_\phi \cdot (\mathbf{u}\times\boldsymbol{\omega} - \nu\nabla\times\boldsymbol{\omega} - \mathbf{g})\, dV$$

$$= -\int dJ \int (\mathbf{u}\times\boldsymbol{\omega} - \nu\nabla\times\boldsymbol{\omega} - \mathbf{g})\cdot d\boldsymbol{\ell}$$

$$= -\frac{1}{2}\int dJ \int \epsilon_{ijk}\Sigma_{ij} d\ell_k \;:=\; \mathscr{T}$$

where $h_\omega = h + \partial_t\phi$ is "rotational pressure" and $dJ = \rho\mathbf{u}_\phi \cdot d\mathbf{A}$ is mass current along potential flow lines. The quantity $\mathscr{T}$ represents energy transfer from potential flow to the rotational flow, defined by $\mathbf{u}_\omega := \mathbf{u} - \mathbf{u}_\phi$:

$$\frac{dE_\phi}{dt} = \int dJ\,(h^{in} - h^{out}) - \mathscr{T}$$

where

$$\frac{dE_\omega}{dt} = \mathscr{T} - \int_\Omega [\eta\,|\boldsymbol{\omega}\,|^2 + \rho\mathbf{u}\cdot\mathbf{g}]\, dV$$

$$E_\phi = (\rho/2)\int_\Omega |\,\mathbf{u}_\phi|^2\, dV, \qquad E_\omega = (\rho/2)\int_\Omega |\,\mathbf{u}_\omega|^2\, dV$$

Vorticity Flux Cospectrum in Wall-Parallel Planes

$$\int_0^\infty dk_x \int_0^\infty dk_z \, (\phi_{v\omega_z}(k_x, k_z, y) - \phi_{w\omega_y}(k_x, k_z, y)) = \langle v\omega_z - w\omega_y \rangle (y)$$

$$y^+ = 20$$

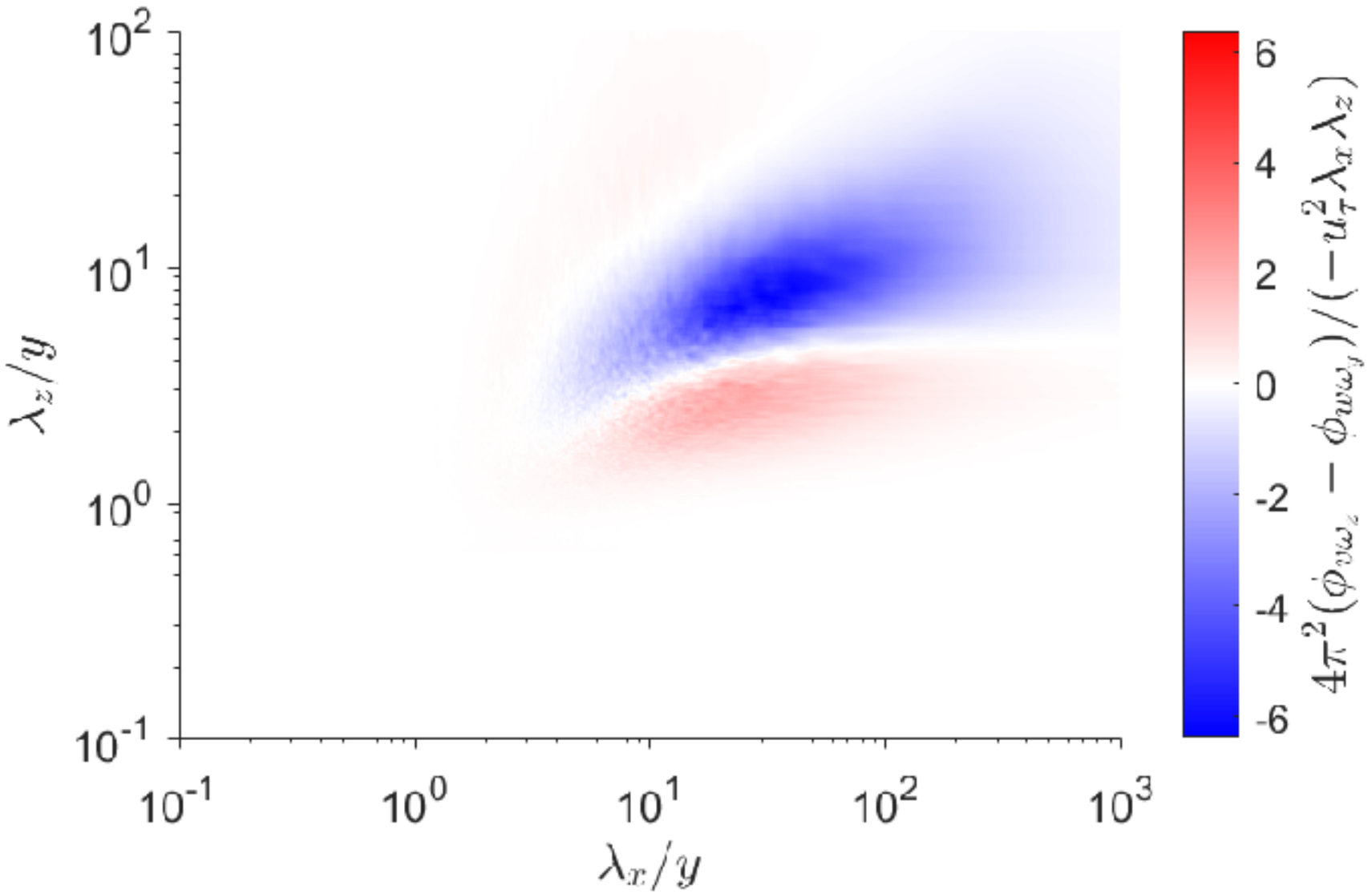

Vorticity Flux Cospectrum in Wall-Parallel Planes

$$\int_0^\infty dk_x \int_0^\infty dk_z \, (\phi_{v\omega_z}(k_x, k_z, y) - \phi_{w\omega_y}(k_x, k_z, y)) = \langle v\omega_z - w\omega_y \rangle (y)$$

$$y^+ = 53$$

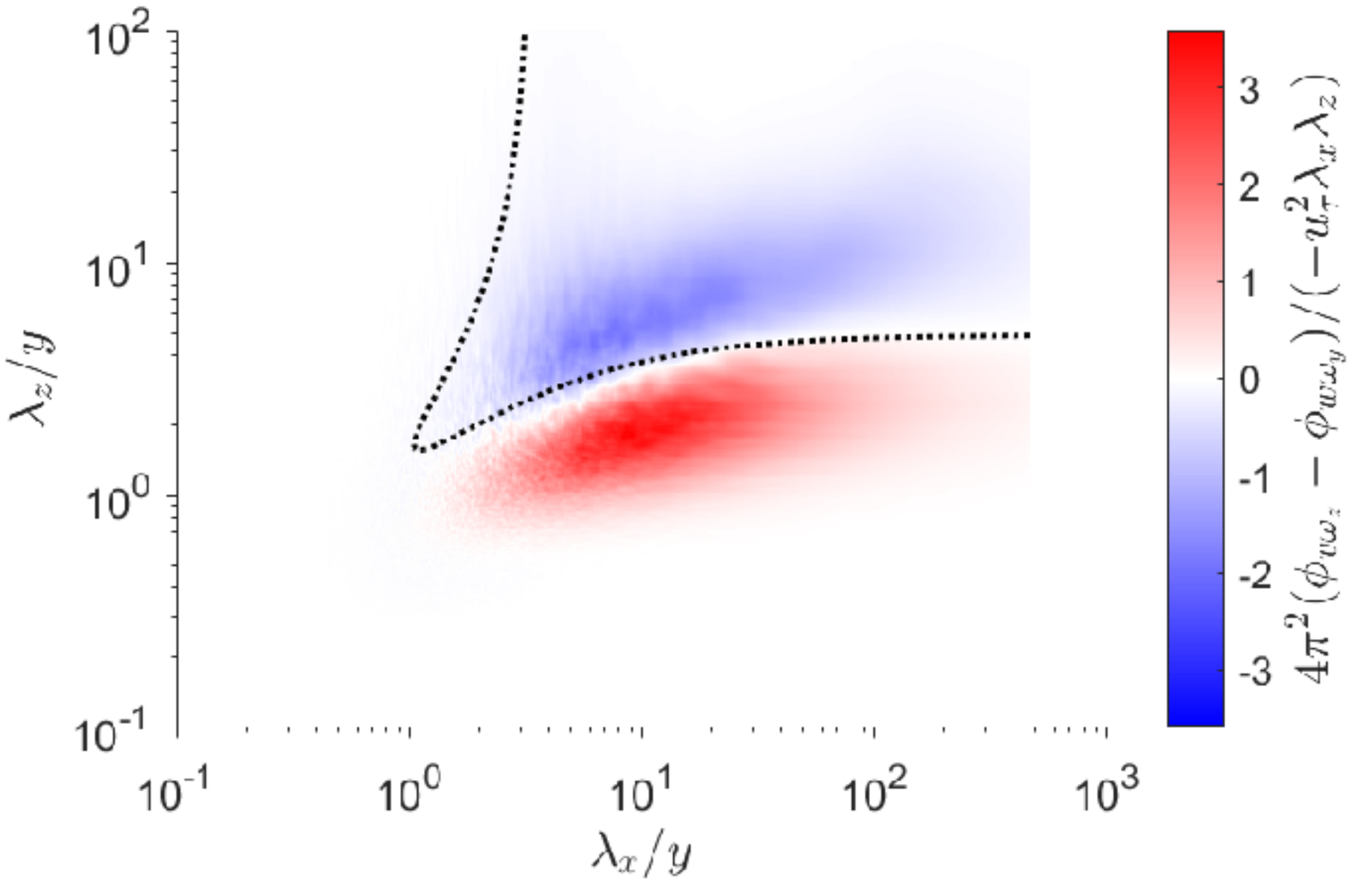

Vorticity Flux Cospectrum in Wall-Parallel Planes

$$\int_0^\infty dk_x \int_0^\infty dk_z \, (\phi_{v\omega_z}(k_x, k_z, y) - \phi_{w\omega_y}(k_x, k_z, y)) = \langle v\omega_z - w\omega_y \rangle(y)$$

$$y^+ = 250$$

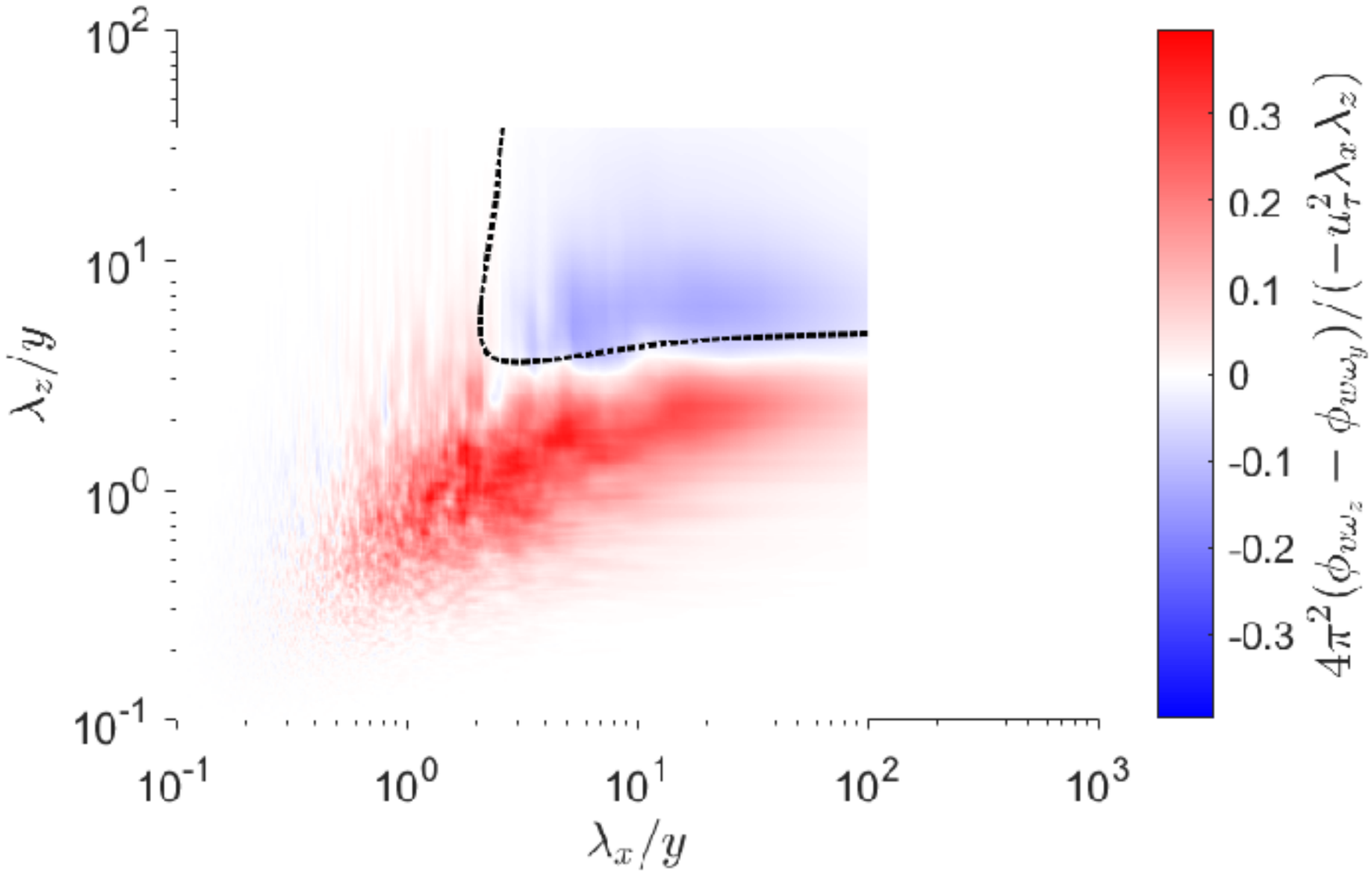

Diffusive Vortical Structures: Attached Eddies

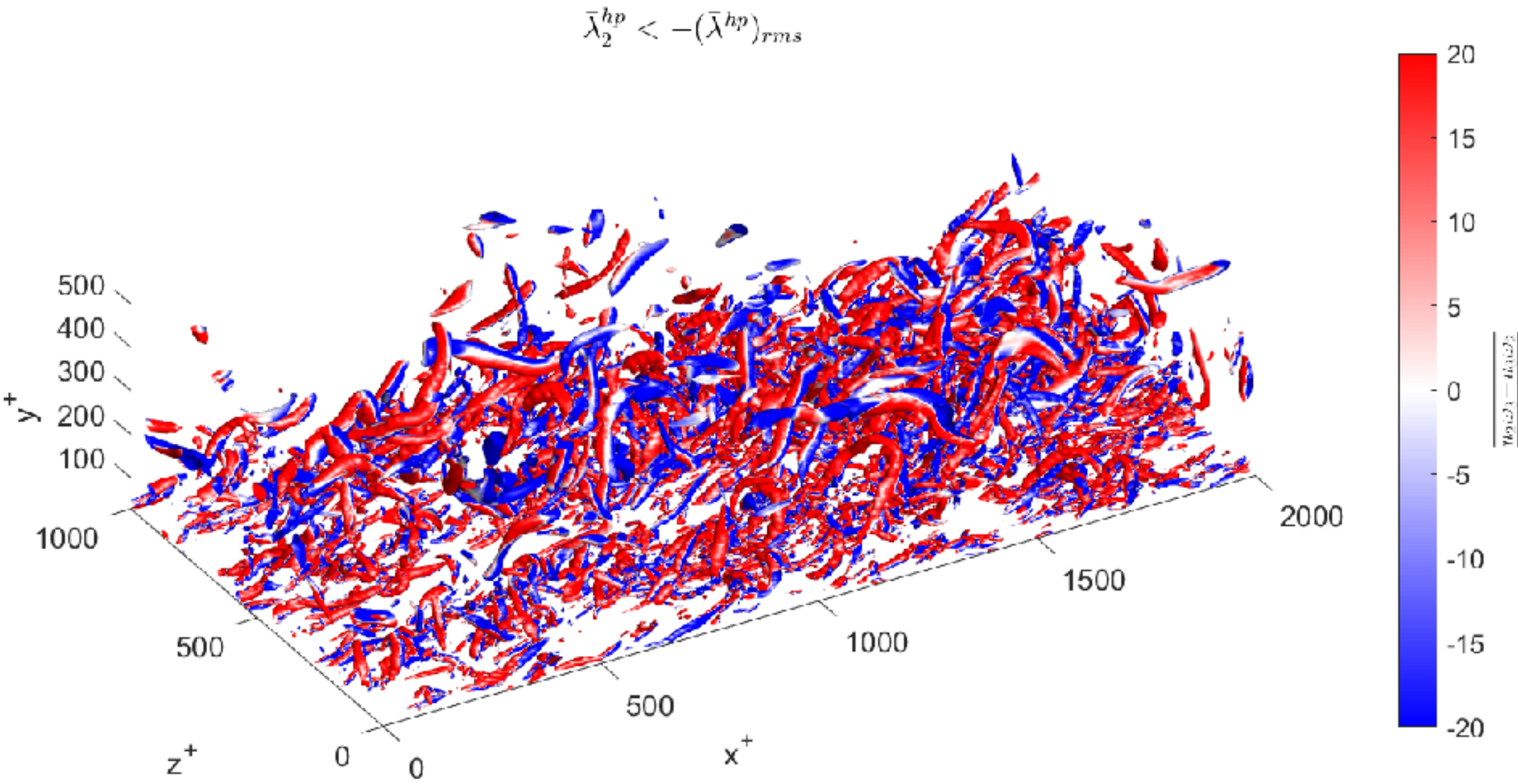

Anti-Diffusive Vortical Structures: Non-Attached Eddies!

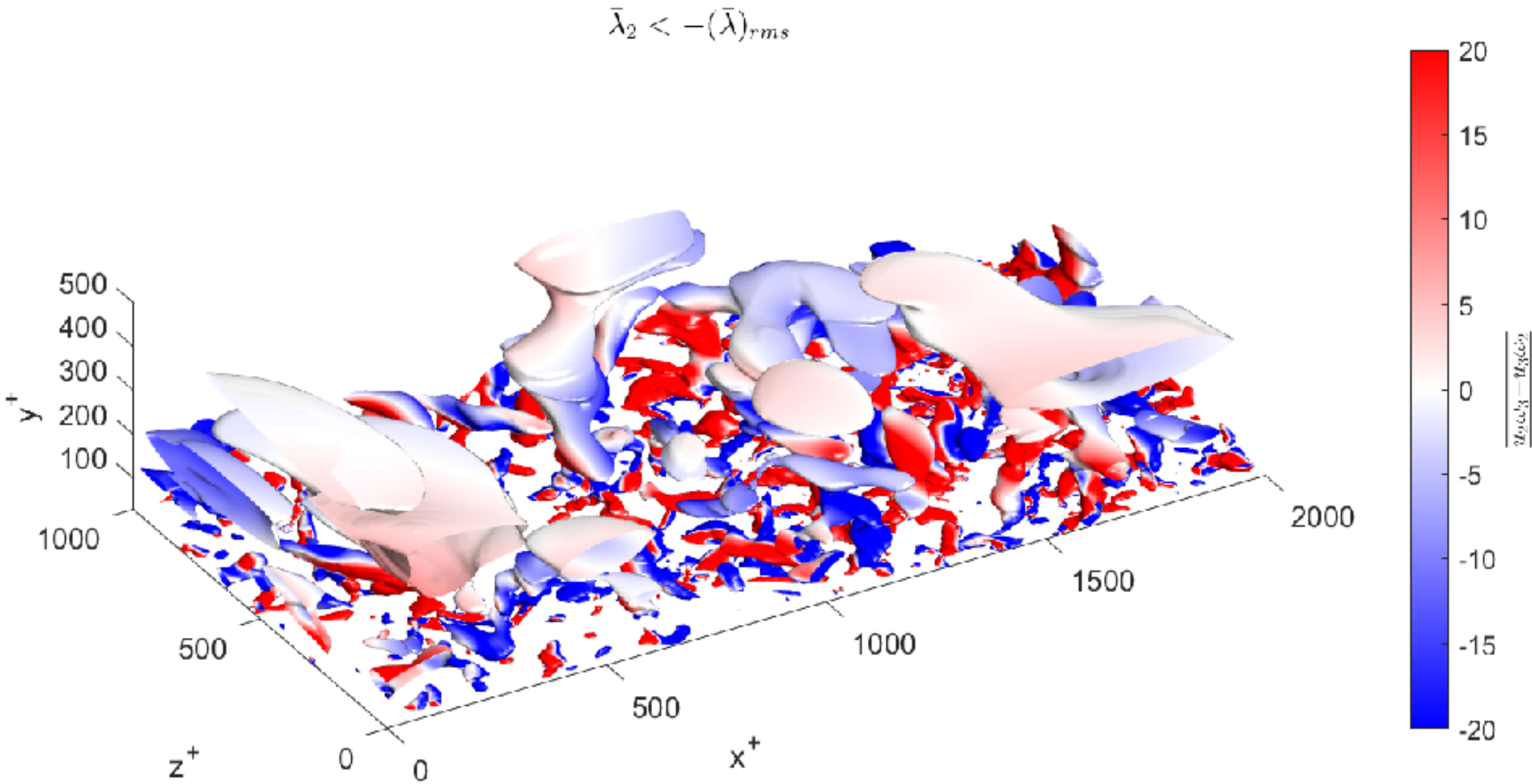

Lighthill (1963) Mechanism of Vorticity Anti-Diffusion

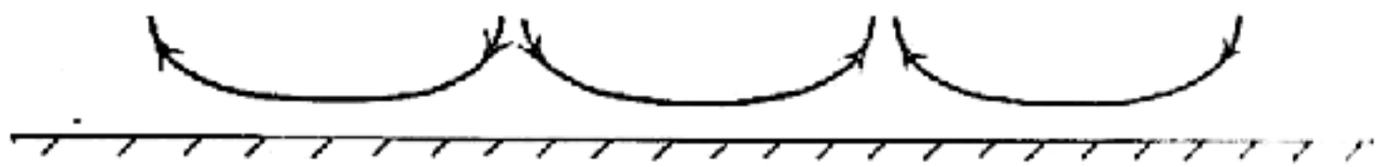

FIG. II. 22. Correlation of inflow with lateral stretching, and outflow with lateral compression, of vortex lines (the mean flow is normal to the plane of the paper).

M. J. Lighthill, in Laminar Boundary Theory, edited by L. Rosenhead (Oxford University Press, Oxford, 1963), pp. 46–113

i. Correlation between turbulent inflow and lateral vortex stretching magnifies principally spanwise vorticity and drives it nearer the wall

ii. Lighthill mechanism of correlated inflow and vortex-stretching is powerfully anti-diffusive, acting against both viscosity and “eddy-viscosity”

iii. Intense competition between anti-diffusive vortex-stretching and diffusion, narrowly won by the latter, since net vorticity must be transferred away under statistically steady condition

iv. Lighthill saw this anti-diffusive transport of vorticity toward the wall as a scale-by-scale cascade process

Importance for Drag Reduction by Polymer Additives

Nonlinear vorticity flux from the wall results from the near-cancellation of two large opposing contributions, thus a slight change in the balance gives large change in drag.

The net diffusive flux is due to contributions from length-scales smaller than the local Taylor microscale, which are particularly sensitive to polymer additives.

Prior work on polymer-vortex interactions:

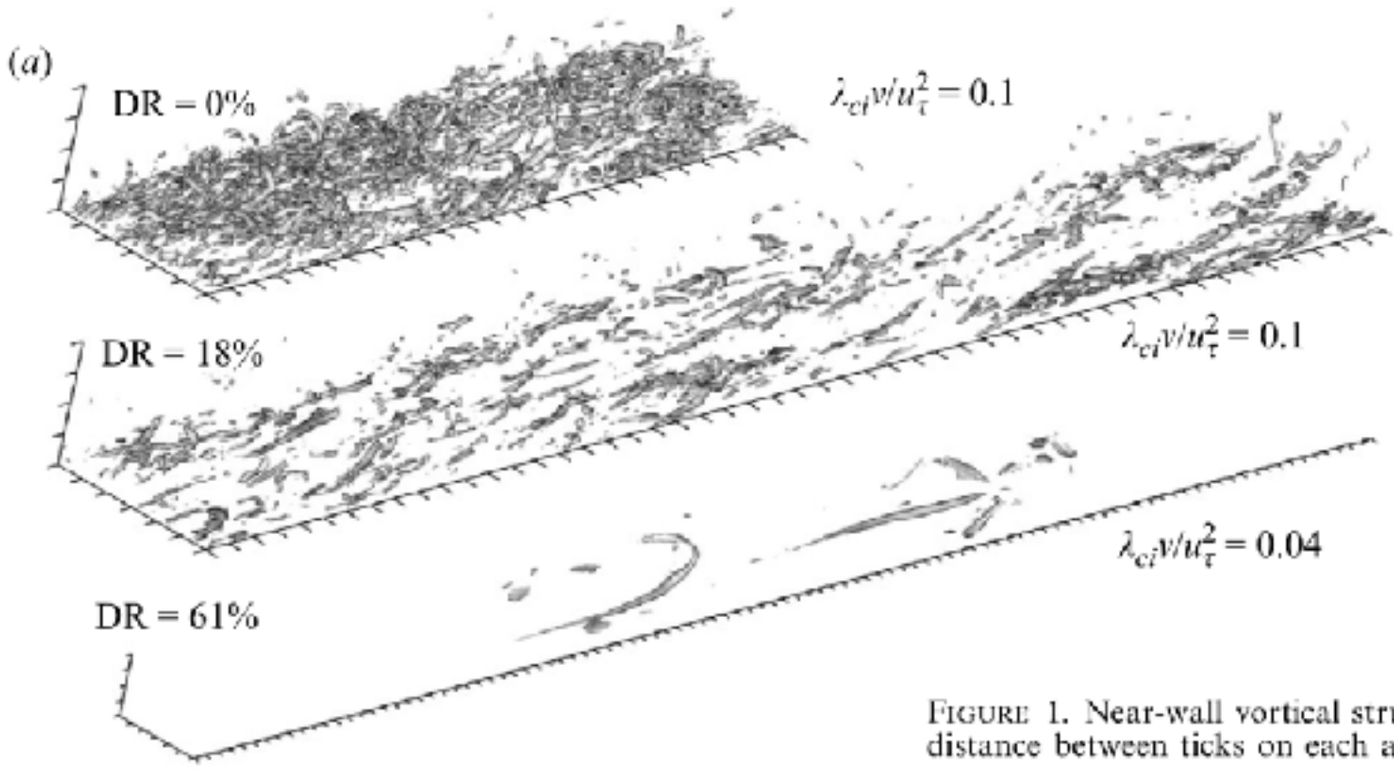

FIGURE 1. Near-wall vortical structure in the drag-reducing flow with polymer additives. The distance between ticks on each axis is 100 wall units.

K. Kim et al. "Effects of polymer stresses on eddy structures in drag-reduced turbulent channel flow," JFM 584: 281–299 (2007)

The JA-relation is the missing link between vorticity dynamics and drag!

Jointly with Tamer Zaki and with grad student Samvit Kumar we are currently calculating wall drag via the JA-relation in a direct comparison of Newtonian turbulent channel flow and polymer-drag reduced channel flow.

References

Published:

Eyink, G. L., Gupta, A., & Zaki, T. A. (2020). Stochastic Lagrangian dynamics of vorticity. Part 1. General theory for viscous, incompressible fluids. Journal of Fluid Mechanics, 901, A2

Eyink, G. L., Gupta, A., & Zaki, T. A. (2020). Stochastic Lagrangian dynamics of vorticity. Part 2. Application to near-wall channel-flow turbulence. Journal of Fluid Mechanics, 901, A3

G. L. Eyink, The Josephson-Anderson relation and the classical D'Alembert paradox, PRX, 11, 031054 (2021)

G. L. Eyink, S. Kumar, and H. Quan, The Onsager theory of wall-bounded turbulence and Taylor's momentum anomaly, Phil. Trans. R. Soc. A 380, 20210079 (2022)

M. Wang, G. L. Eyink and T. A. Zaki, Origin of enhanced skin friction at the onset of boundary-layer transition, JFM, 941, A32 (2022)

Submitted:

H. Quan and G. L. Eyink, Inertial momentum dissipation for viscosity solutions of Euler equations. I. Flow around a smooth body, Communications in Mathematical Physics, submitted; https://arxiv.org/abs/2206.05325

H. Quan and G. L. Eyink, Onsager theory of turbulence, the Josephson-Anderson relation, and the D'Alembert paradox, Communications in Mathematical Physics, submitted; https://arxiv.org/abs/2206.05326

In Progress:

S. Kumar, C. Meneveau and G. L. Eyink, Vorticity cascade and turbulent drag in wall-bounded flows: plane Poiseuille flow.

S. Kumar and G. L. Eyink, Turbulent drag in generalized channel flows and the Josephson-Anderson relation

S. Kumar, T. Zaki, and G. L. Eyink, Turbulent drag-reduction by polymer additives and the Josephson-Anderson relation

H. Quan and G. L. Eyink, Strong-weak uniqueness and flow around Impulsively-accelerated bodies

G. L. Eyink, Onsager theory of wall-bounded flow and the turbulent vorticity cascade

Huggins Vorticity Current Tensor

Huggins (1970,1971) starts with the incompressible Navier-Stokes equation, including an external potential U (e.g. gravity) and a non-potential force $\mathbf{g}$ (e.g. polymer stress):

$$\partial_t \mathbf{u} = \mathbf{u}\times\boldsymbol{\omega} - \nu\boldsymbol{\nabla}\times\boldsymbol{\omega} - \mathbf{g} - \boldsymbol{\nabla}\left(p + U + \frac{1}{2}|\mathbf{u}|^2\right)$$

Huggins rewrote this as

$$\partial_t u_i = \frac{1}{2}\epsilon_{ijk}\Sigma_{jk} - \partial_i h$$

where $h = p + U + \frac{1}{2}|\mathbf{u}|^2$ is a generalized enthalpy (or total pressure) and

$$\Sigma_{ij} = u_i\omega_j - u_j\omega_i + \nu\left(\frac{\partial\omega_i}{\partial x_j} - \frac{\partial\omega_j}{\partial x_i}\right) - \epsilon_{ijk}g_k$$

is an anti-symmetric vorticity current tensor which represents flux of j-component of vorticity in the coordinate i-direction $\partial_t\omega_j + \partial_i\Sigma_{ij} = 0$. It is related to Lighthill's "vorticity source vector" $\boldsymbol{\sigma}$ by

$$\boldsymbol{\sigma} = \hat{\mathbf{n}}\cdot\boldsymbol{\Sigma} = -\hat{\mathbf{n}}\times(\boldsymbol{\nabla}h + \partial_t\mathbf{u})$$

which it extends into the flow interior. A mean gradient in h implies mean vorticity flux:

$$\overline{\Sigma}_{ij} = \epsilon_{ijk}\partial_k\overline{h}$$

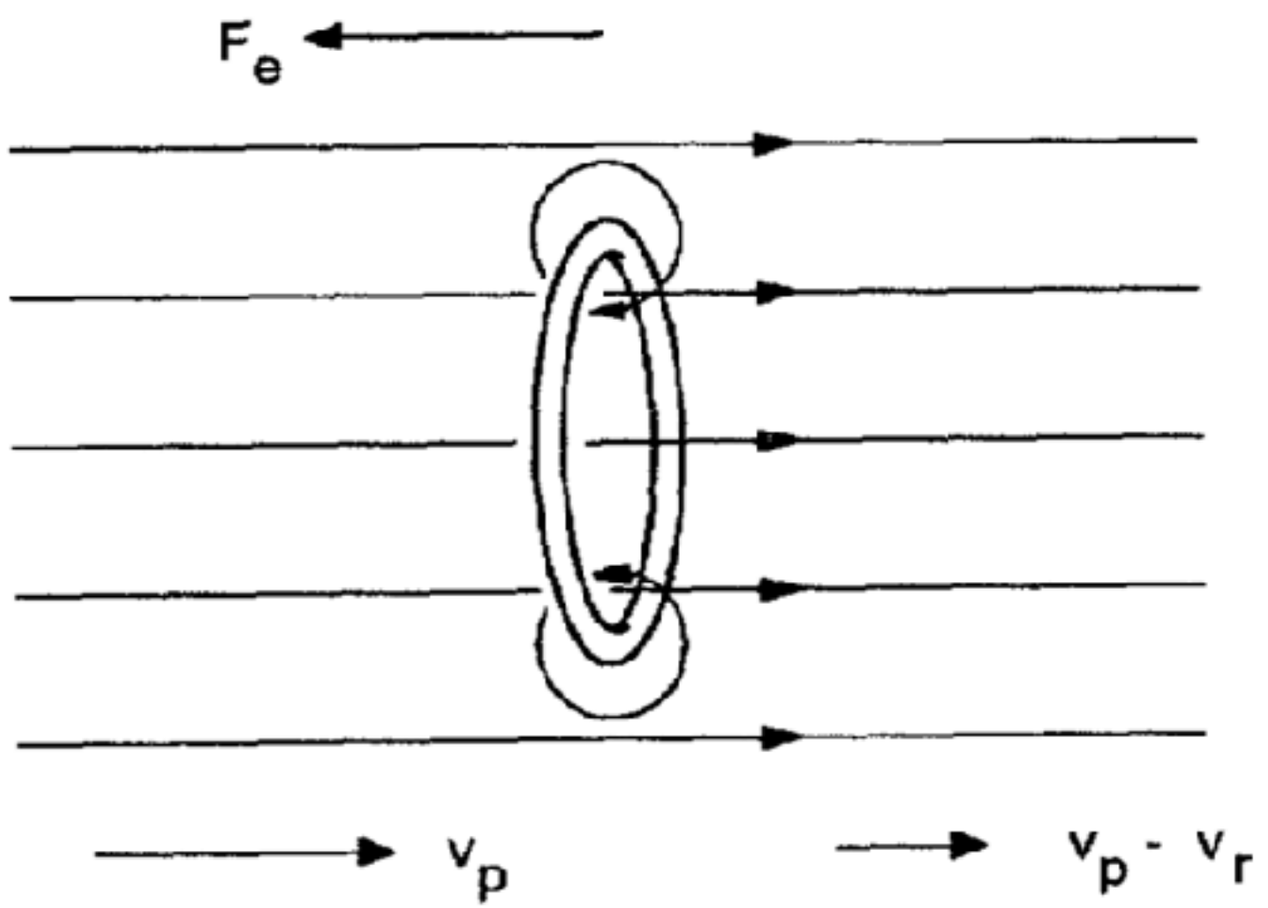

Fig. 3.1. Example A: A circular vortex ring with self-induced velocity v_r to the left is being swept to the right in a uniform potential flow field v_p, with $v_p > v_r$. A resistive force F_e acts on the vortex core to the left, causing the radius of the ring to grow.

From W. Zimmermann, Jr. “Energy Transfer and Phase Slip by Quantum Vortex Motion in Superfluid ^{4}He,” Journal of Low Temperature Physics, Vol. 93, Nos. 5/6, 1993

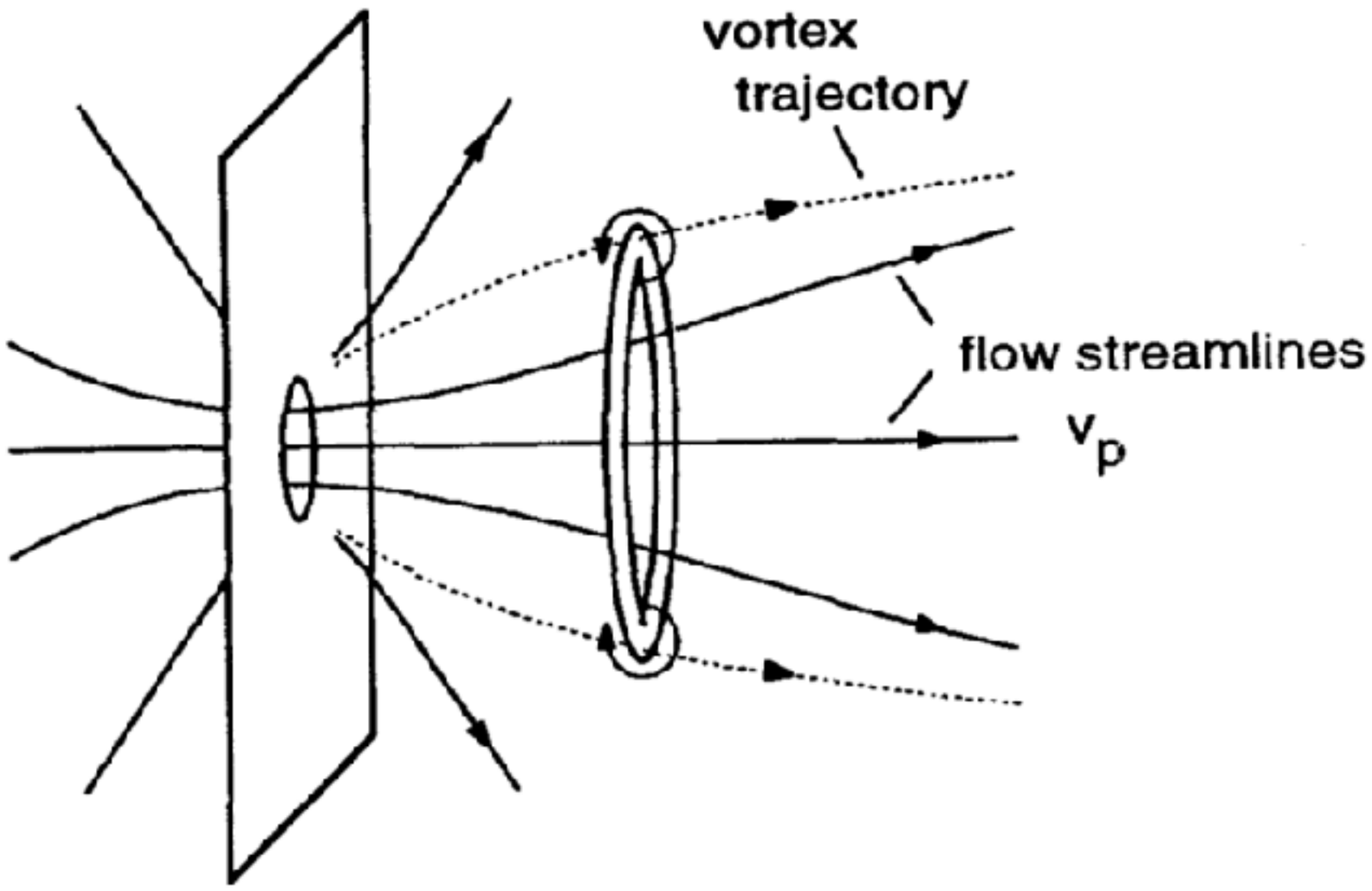

Fig. 3.2. Example B: A circular vortex ring with self-induced velocity to the right moves in a potential flow field directed to the right and diverging from an orifice in a plane wall. The dotted curves show a calculated representative trajectory for the core of the ring.

Application to Turbulent Channel-Flow

E. R. Huggins, “Vortex currents in turbulent superfluid and classical fluid channel flow, the Magnus effect, and Goldstone boson fields,” J. Low Temp. Phys. 96, 317–346 (1994).

Gregory L Eyink, “Turbulent flow in pipes and channels as cross-stream ‘inverse cascades’ of vorticity,” Physics Fluids 20, 125101 (2008).

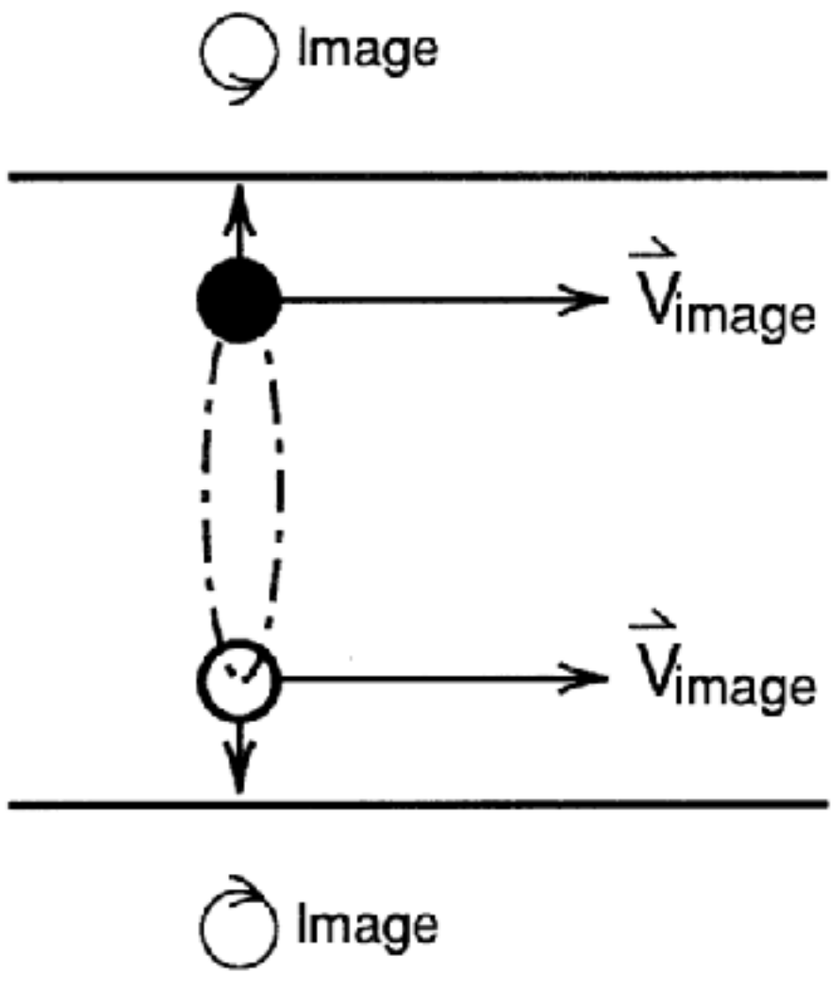

Fig. 8. Picture superfluid helium flowing through a gas of essentially stationary excitations. The vortex ring has expanded to the point shown above due to fluctuations or eddy viscosity. At this point the image velocity begins to move the ring rapidly downstream, through the stationary excitations. The scattering of the excitations creates a left directed non-potential force which expands the ring into the wall. (To see this expansion is a good exercise in the use of Fig. 1.)

For classical turbulence in a pipe, vortex rings of opposite circulation instead shrink to the center and annihilate!

Flow Past a Finite Solid Body

G. Eyink, “The Josephson-Anderson Relation and the Classical D’Alembert Paradox,”

https://arxiv.org/abs/2103.15177

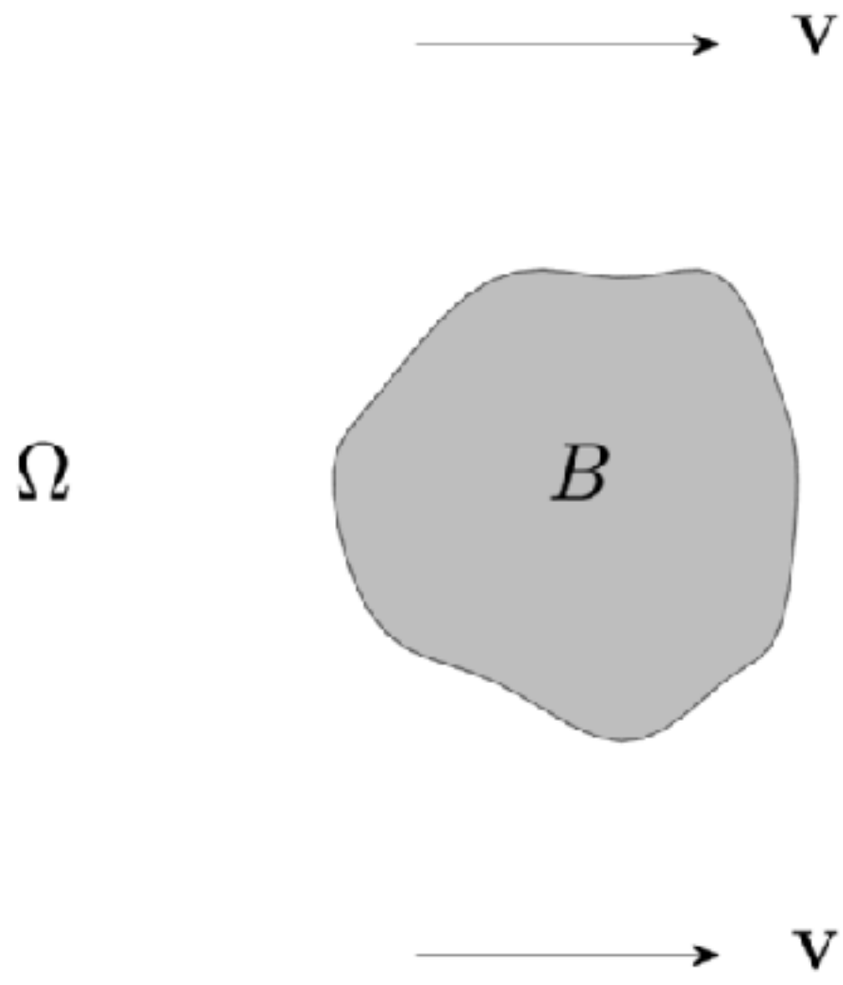

FIG. 2 Flow around a finite body B in an unbounded region Ω filled with fluid moving at a velocity $\mathbf{V}$ at far distances.

Ideal Euler Flow Past a Solid Body

The potential solution of the incompressible Euler equation for flow past body B

$$\partial_t \mathbf{u}_\phi + \boldsymbol{\nabla}\cdot(\mathbf{u}_\phi \mathbf{u}_\phi + p_\phi \mathbf{I}) = \mathbf{0}, \quad \boldsymbol{\nabla}\cdot\mathbf{u}_\phi = 0$$

can be solved for the velocity potential ϕ in $\mathbf{u}_\phi = \boldsymbol{\nabla}\phi$ from the Laplace problem

$$\triangle\phi = 0 \qquad \left.\frac{\partial\phi}{\partial n}\right|_{\partial B} = 0, \quad \phi \underset{|\mathbf{x}|\to\infty}{\sim} \mathrm{V}x$$

with kinematic pressure p_ϕ given by the Bernoulli equation

$$\partial_t\phi + \frac{1}{2}|\mathbf{u}_\phi|^2 + p_\phi = const.$$

The force that the fluid exerts on the body arises from pressure $P_\phi = \rho p_\phi$

$$\mathbf{F}_\phi = -\int_{\partial B} P_\phi\, \hat{\mathbf{n}}\, dA$$

and by d'Alembert's result has vanishing drag component, $\mathbf{V}\cdot\mathbf{F}_\phi = 0$.

The Detailed Josephson-Anderson Relation for Flow Past a Body

For the incompressible Navier-Stokes solution, the reaction force of the body back on the fluid

$$\mathbf{F} = \int_{\partial B} (P\ \hat{\mathbf{n}} + 2\eta \mathbf{S}\hat{\mathbf{n}}) dA$$

is given by

$$\begin{aligned} -\mathbf{F}\cdot\mathbf{V} &= -\rho \int_{\Omega} \mathbf{u}_\phi \cdot (\mathbf{u}\times\boldsymbol{\omega} - \nu\boldsymbol{\nabla}\times\boldsymbol{\omega}) dV \\ &= -\int dJ \int (\mathbf{u}\times\boldsymbol{\omega} - \nu\boldsymbol{\nabla}\times\boldsymbol{\omega})\cdot d\boldsymbol{\ell} \\ &= -\frac{1}{2}\int dJ \int \epsilon_{ijk}\Sigma_{ij} d\ell_k, \end{aligned}$$

Defining the velocity of the rotational wake, $\mathbf{u}_\omega = \mathbf{u} - \mathbf{u}_\phi$, the relation again represents energy transfer between potential and rotational flow:

$$\frac{dE_{int}}{dt} = +\rho \int_{\Omega} \mathbf{u}_\phi \cdot (\mathbf{u}\times\boldsymbol{\omega} - \nu\boldsymbol{\nabla}\times\boldsymbol{\omega}) dV,$$

$$\frac{dE_{\omega}}{dt} = -\rho \int_{\Omega} \mathbf{u}_\phi \cdot (\mathbf{u}\times\boldsymbol{\omega} - \nu\boldsymbol{\nabla}\times\boldsymbol{\omega})\, dV - \int_{\Omega} \eta |\omega|^2\, dV$$

with

$$E_{int}(t) = \rho \int_{\Omega} \mathbf{u}_\omega(\mathbf{x},t)\cdot\mathbf{u}_\phi(\mathbf{x},t)\, dV \qquad E_{\omega}(t) = \frac{1}{2}\rho \int_{\Omega} |\mathbf{u}_\omega(\mathbf{x},t)|^2\, dV,$$

The Detailed Josephson-Anderson Relation for Flow Past a Body

For the incompressible Navier-Stokes solution, the reaction force of the body back on the fluid

$$\mathbf{F} = \int_{\partial B} (P\ \hat{\mathbf{n}} + 2\eta \mathbf{S}\hat{\mathbf{n}}) dA$$

is given by

$$\begin{aligned} -\mathbf{F}\cdot\mathbf{V} &= -\rho \int_{\Omega} \mathbf{u}_\phi \cdot (\mathbf{u}\times\boldsymbol{\omega} - \nu\boldsymbol{\nabla}\times\boldsymbol{\omega}) dV \\ &= -\int dJ \int (\mathbf{u}\times\boldsymbol{\omega} - \nu\boldsymbol{\nabla}\times\boldsymbol{\omega})\cdot d\boldsymbol{\ell} \\ &= -\frac{1}{2}\int dJ \int \epsilon_{ijk}\Sigma_{ij} d\ell_k, \end{aligned}$$

Defining the velocity of the rotational wake, $\mathbf{u}_\omega = \mathbf{u} - \mathbf{u}_\phi$, the relation again represents energy transfer between potential and rotational flow:

$$\frac{dE_{int}}{dt} = +\rho \int_{\Omega} \mathbf{u}_\phi \cdot (\mathbf{u}\times\boldsymbol{\omega} - \nu\boldsymbol{\nabla}\times\boldsymbol{\omega}) dV,$$

$$\frac{dE_{\omega}}{dt} = -\rho \int_{\Omega} \mathbf{u}_\phi \cdot (\mathbf{u}\times\boldsymbol{\omega} - \nu\boldsymbol{\nabla}\times\boldsymbol{\omega})\, dV - \int_{\Omega} \eta |\omega|^2\, dV$$

with

$$E_{int}(t) = \rho \int_{\Omega} \mathbf{u}_\omega(\mathbf{x},t)\cdot\mathbf{u}_\phi(\mathbf{x},t)\, dV \qquad E_{\omega}(t) = \frac{1}{2}\rho \int_{\Omega} |\mathbf{u}_\omega(\mathbf{x},t)|^2\, dV,$$

Ideal Flow Past a Sphere

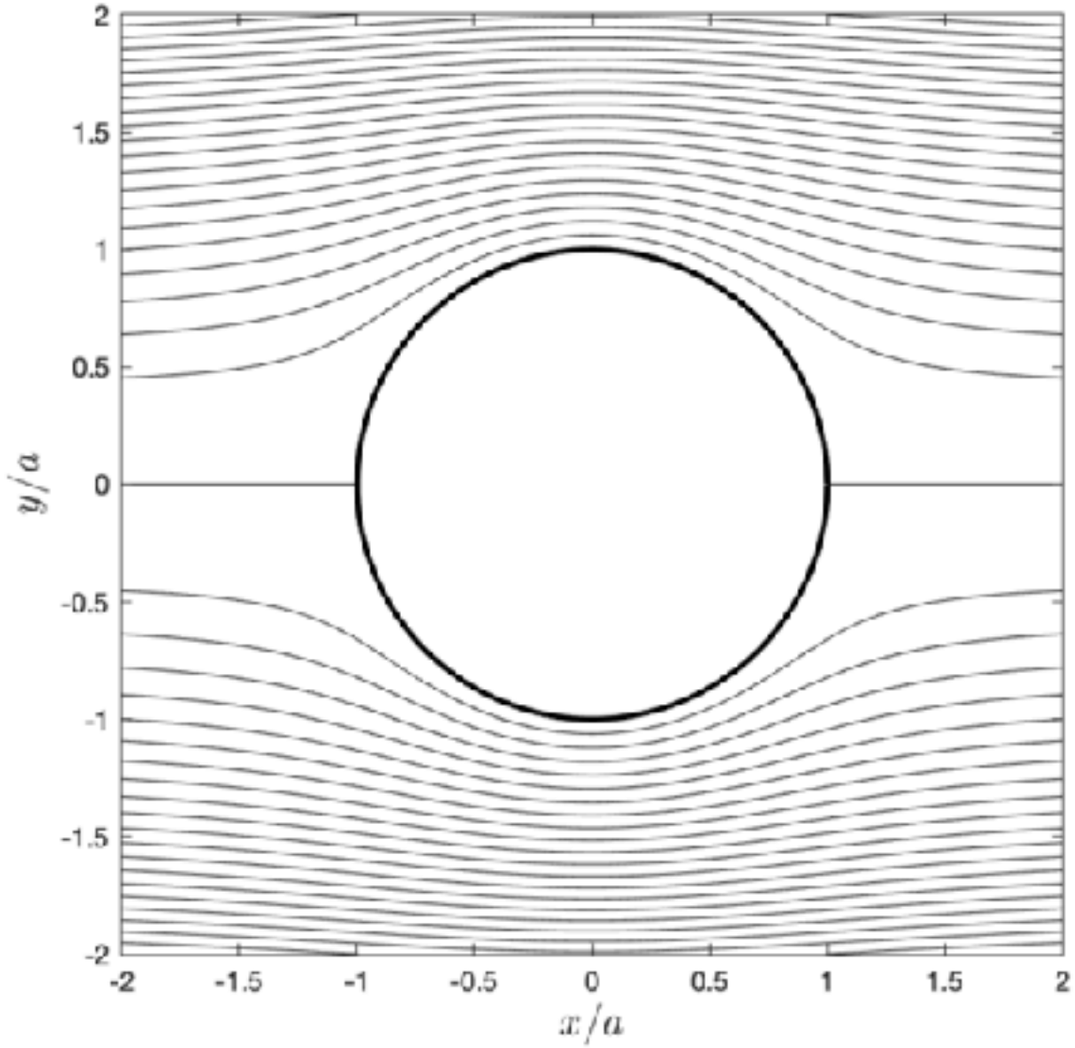

Streamlines of ideal flow around a sphere, levels sets of the Stokes stream-function:

$$\psi = \frac{1}{2} V r^2 \sin^2\theta \left(1 - \frac{a^3}{r^3}\right)$$
$$= \frac{1}{2} V \sigma^2 \left[1 - \frac{a^3}{(\sigma^2 + x^2)^{3/2}}\right] \qquad \sigma = \sqrt{y^2 + z^2}$$

The lines are polar at the sphere surface, but become axial within a distance from the sphere of about one radius at most. Note also that $dJ = \rho\, d\psi\, d\varphi$.

Schematic "Cartoon" of Drag on a Sphere

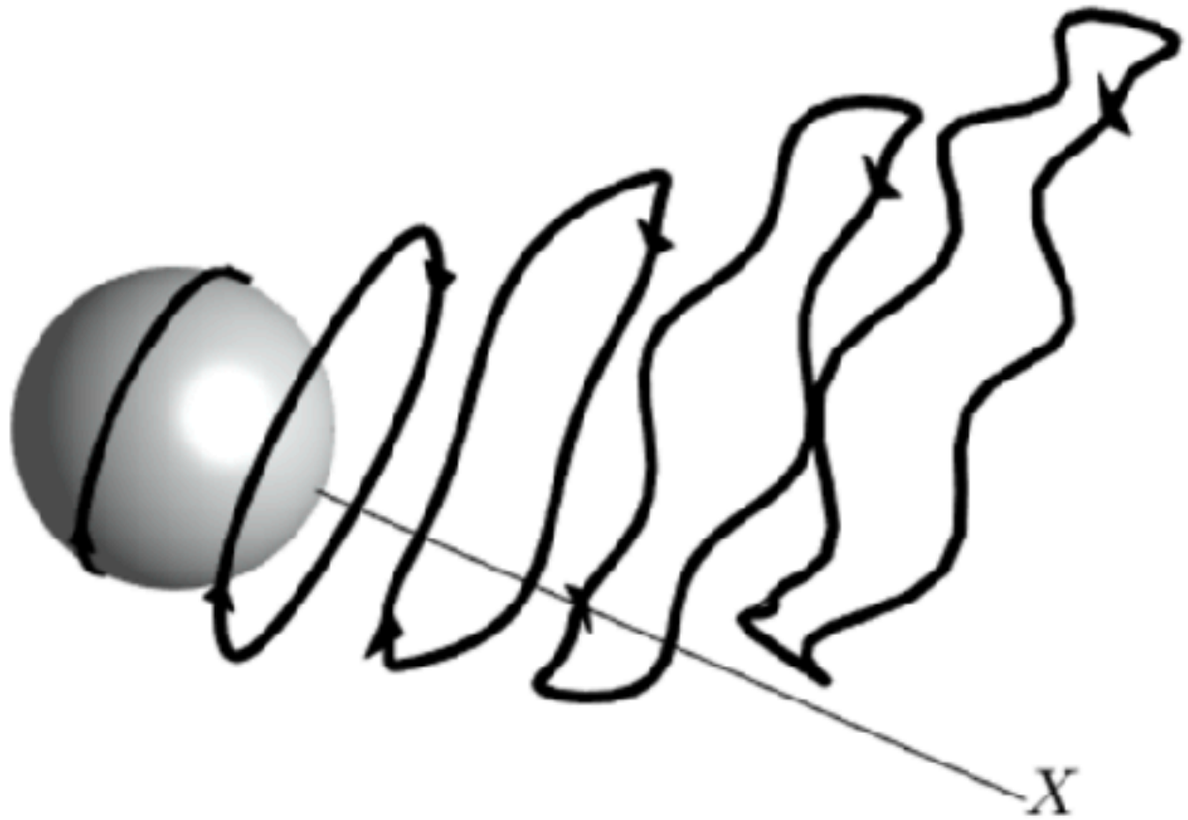

FIG. 5 Rough cartoon of the drag mechanism by generation and outward flux of vortex loops with negative azimuthal vorticity. The rings are generated by pressure drop along the surface. As the rings expand outward, they enclose greater mass flux J and subtract proportionate energy from the potential flow. Although the rings initially loop around the streamwise axis X, they drift across in time. This implies a flux of azimuthal vorticity across X and allows the pressure to recover far downstream from its drop around the sphere.

Vorticity Conservation

In any plane through the axis of the sphere, with unit normal $\hat{\mathbf{N}}$, the vorticity through the plane must be locally conserved:

$$\partial_t \omega_n + \boldsymbol{\nabla}\cdot\mathbf{j}_n = 0$$

where

$$\omega_n = \boldsymbol{\omega}\cdot\hat{\mathbf{N}}, \quad \mathbf{j}_n = \boldsymbol{\Sigma}\cdot\hat{\mathbf{N}}$$

Thus, $\nabla\cdot\langle\mathbf{j}_n\rangle=0$.

Note in the upper half-plane

$$\hat{\mathbf{N}} = \hat{\boldsymbol{\varphi}}$$

and in the lower half-plane

$$\hat{\mathbf{N}} = -\hat{\boldsymbol{\varphi}}$$

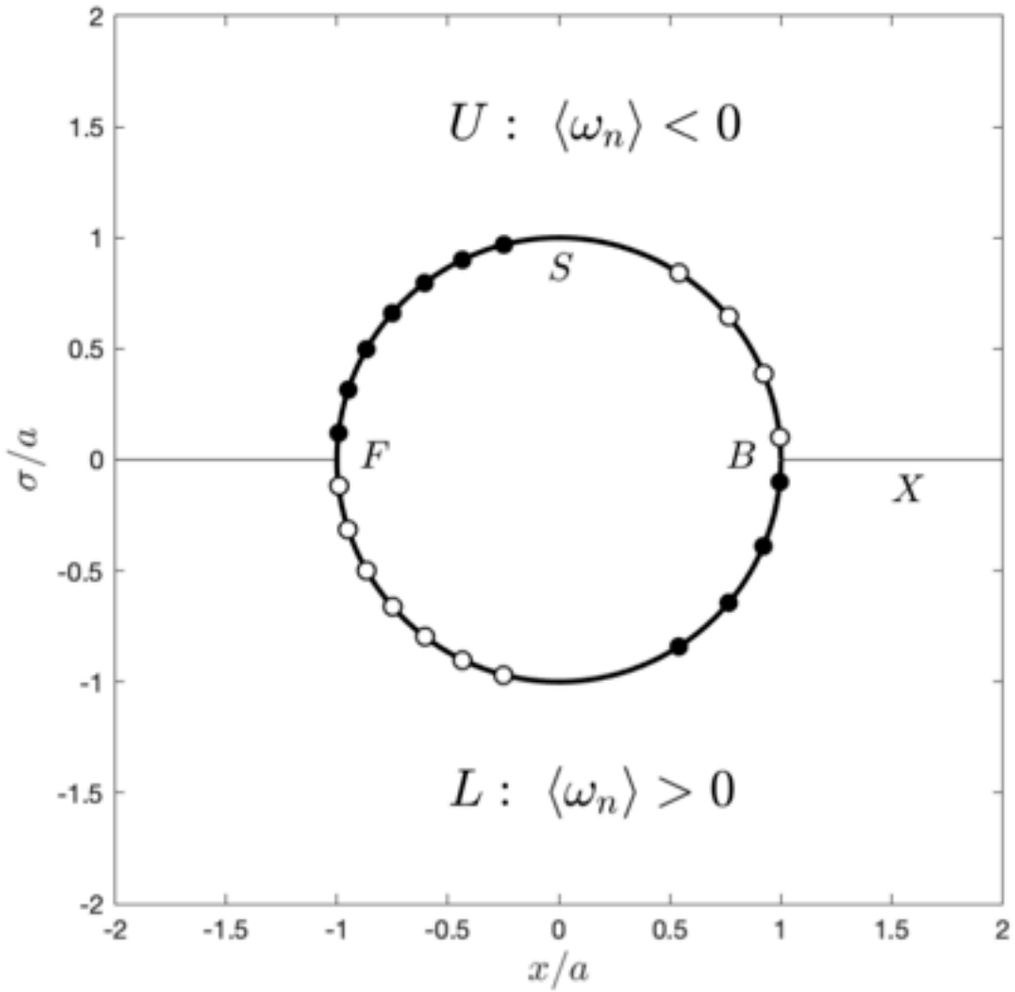

FIG. 4 Schematic of azimuthal vorticity generation on the surface of the sphere. Following the convention of Huggins [13], we use white circles to denote vorticity out of the plane ($\omega_n > 0$) and black circles to denote vorticity into the plane ($\omega_n < 0$). The mean normal (azimuthal) vorticity in the upper half-plane U is negative and the mean normal (anti-azimuthal) vorticity in the lower half-plane L is positive, implying a pole-to-pole asymmetry in the pressure distribution on the surface S of the sphere. The pressure drop along the surface of the sphere from F to B is exactly compensated by the pressure rise from B to infinity along the direction of the positive streamwise axis X.

Vorticity Conservation

In any plane through the axis of the sphere, with unit normal $\hat{\mathbf{N}}$, the vorticity through the plane must be locally conserved:

$$\partial_t \omega_n + \boldsymbol{\nabla}\cdot\mathbf{j}_n = 0$$

where

$$\omega_n = \boldsymbol{\omega}\cdot\hat{\mathbf{N}}, \quad \mathbf{j}_n = \boldsymbol{\Sigma}\cdot\hat{\mathbf{N}}$$

Thus, $\boldsymbol{\nabla}\cdot\langle\mathbf{j}_n\rangle=0$.

Note in the upper half-plane

$$\hat{\mathbf{N}} = \hat{\boldsymbol{\varphi}}$$

and in the lower half-plane

$$\hat{\mathbf{N}} = -\hat{\boldsymbol{\varphi}}$$

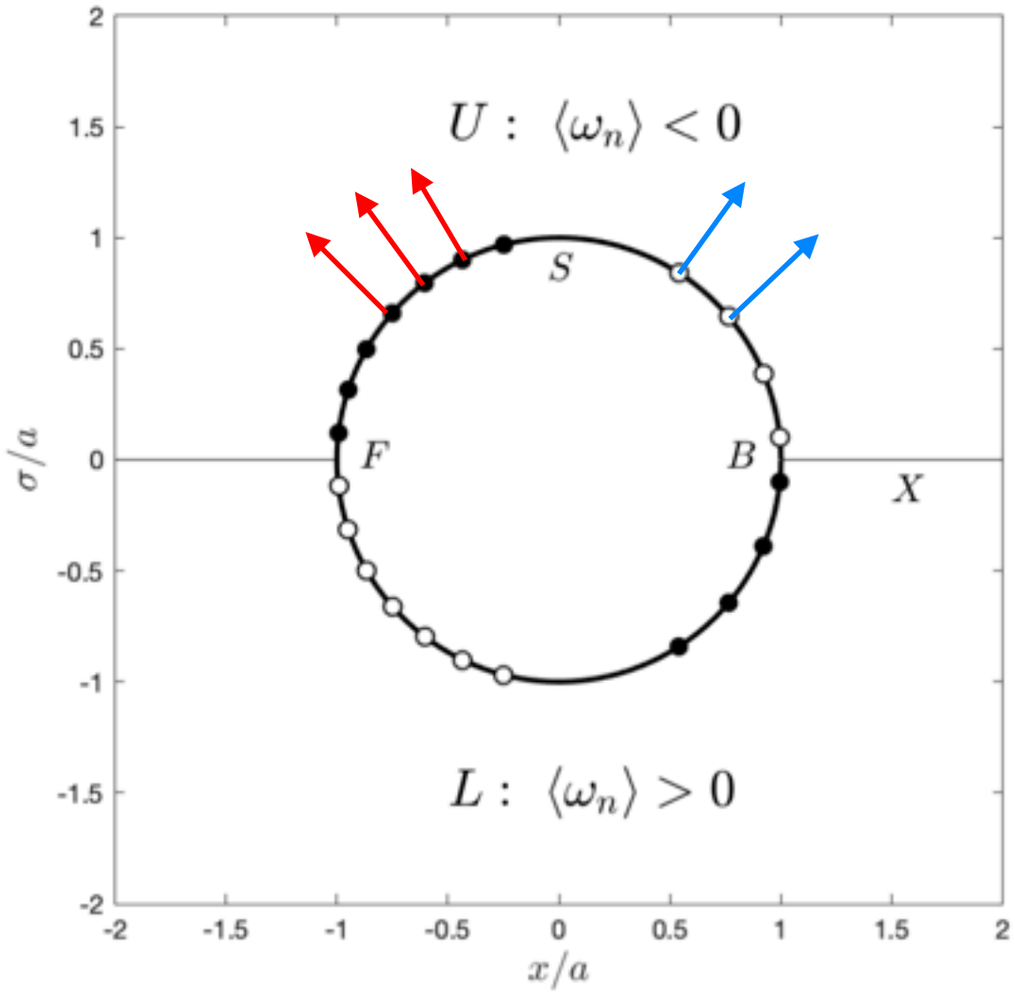

FIG. 4 Schematic of azimuthal vorticity generation on the surface of the sphere. Following the convention of Huggins [13], we use white circles to denote vorticity out of the plane ($\omega_n > 0$) and black circles to denote vorticity into the plane ($\omega_n < 0$). The mean normal (azimuthal) vorticity in the upper half-plane U is negative and the mean normal (anti-azimuthal) vorticity in the lower half-plane L is positive, implying a pole-to-pole asymmetry in the pressure distribution on the surface S of the sphere. The pressure drop along the surface of the sphere from F to B is exactly compensated by the pressure rise from B to infinity along the direction of the positive streamwise axis X.

Vorticity Conservation

In any plane through the axis of the sphere, with unit normal $\hat{\mathbf{N}}$, the vorticity through the plane must be locally conserved:

$$\partial_t \omega_n + \boldsymbol{\nabla}\cdot\mathbf{j}_n = 0$$

where

$$\omega_n = \boldsymbol{\omega}\cdot\hat{\mathbf{N}}, \quad \mathbf{j}_n = \boldsymbol{\Sigma}\cdot\hat{\mathbf{N}}$$

Thus, $\nabla\cdot\langle\mathbf{j}_n\rangle=0$.

Note in the upper half-plane

$$\hat{\mathbf{N}} = \hat{\boldsymbol{\varphi}}$$

and in the lower half-plane

$$\hat{\mathbf{N}} = -\hat{\boldsymbol{\varphi}}$$

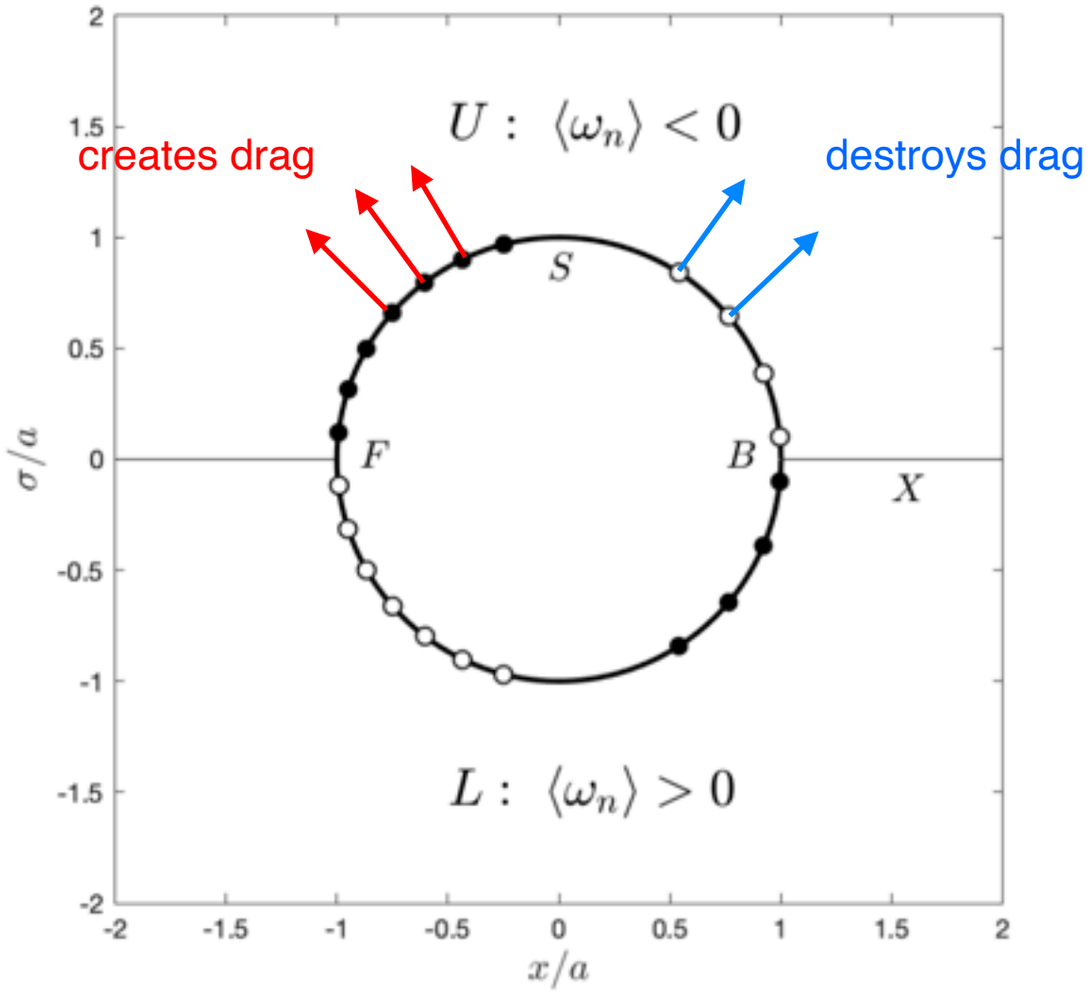

FIG. 4 Schematic of azimuthal vorticity generation on the surface of the sphere. Following the convention of Huggins [13], we use white circles to denote vorticity out of the plane ($\omega_n > 0$) and black circles to denote vorticity into the plane ($\omega_n < 0$). The mean normal (azimuthal) vorticity in the upper half-plane U is negative and the mean normal (anti-azimuthal) vorticity in the lower half-plane L is positive, implying a pole-to-pole asymmetry in the pressure distribution on the surface S of the sphere. The pressure drop along the surface of the sphere from F to B is exactly compensated by the pressure rise from B to infinity along the direction of the positive streamwise axis X.

Drag Creation by Outward Flux of Vorticity

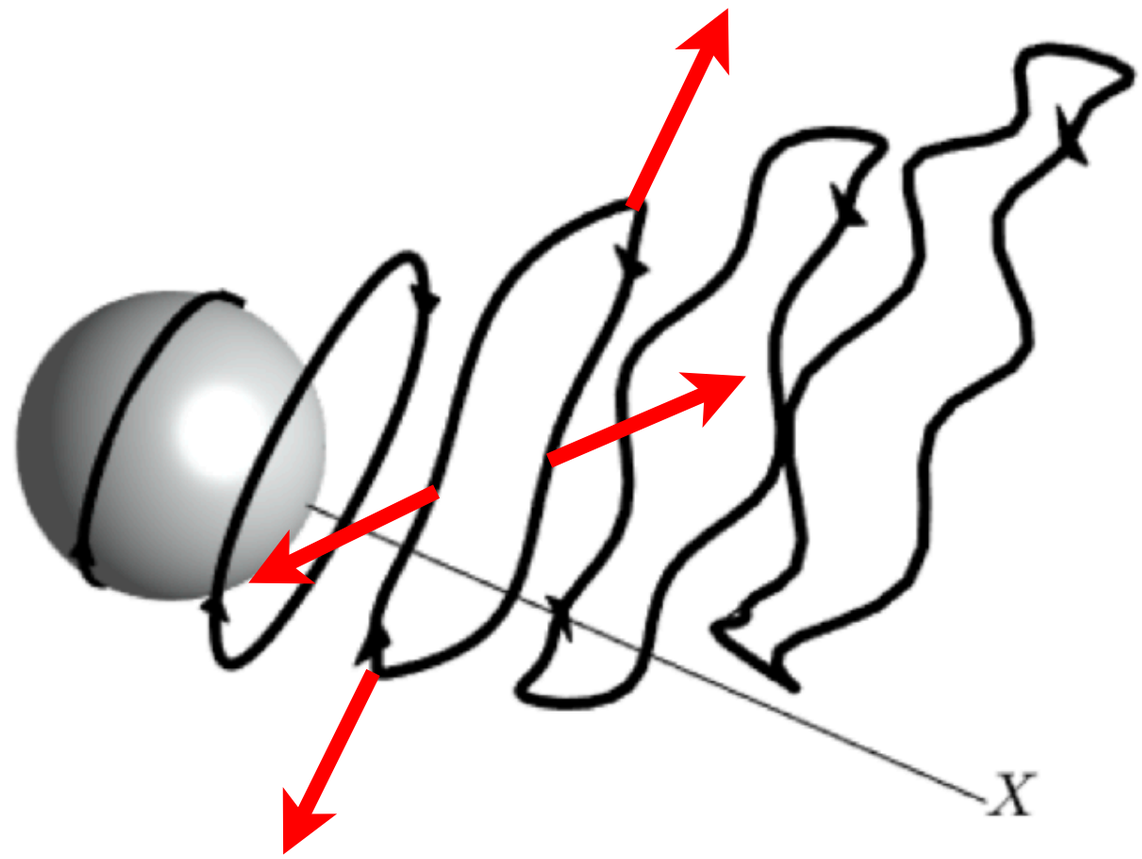

Away from the sphere, drag results from flux of negative ω_φ in the σ-direction and flux of positive ω_σ in the φ-direction, which are linked by $\Sigma_{\sigma\varphi}$=-$\Sigma_{\varphi\sigma}$.

The streamwise vorticity ω_x and its flux make no contribution to drag!

The vortex loops drift across the X-axis, unlinking from it and thus restoring the pressure far downstream to its original value upstream.

Resolution of the Modern D'Alembert Paradox

The mechanism of drag by the JA-relation is independent of Reynolds number and holds both for $Re \ll 1$ and for $Re \gg 1$.

Does it hold also for $Re \to \infty$? *A priori* the term $\mathbf{u}_\omega \times \boldsymbol{\omega}$ appearing in the JA-relation is ill-defined at infinite Reynolds number. However, the standard identity

$$\mathbf{u}_\omega \times \boldsymbol{\omega} = -\boldsymbol{\nabla} \cdot \left[\mathbf{u}_\omega \mathbf{u}_\omega - \frac{1}{2} |\mathbf{u}_\omega|^2 \mathbf{I} \right]$$

allows to rewrite the inertial term in the JA-relation instead as

$$\int_\Omega \mathbf{u}_\phi \cdot (\mathbf{u}_\omega \times \boldsymbol{\omega})\, dV = \int_\Omega \boldsymbol{\nabla} \mathbf{u}_\phi : \mathbf{u}_\omega \mathbf{u}_\omega \, dV$$

and in this form it is well-defined as long as $\mathbf{u}_\omega \in L^2$. *This remarks suggests that the JA-relation should hold for limiting weak Euler solutions obtained as* $Re \to \infty$.

This problem can be investigated with the Onsager RG-methods developed for wall-bounded flows, as discussed previously for turbulent channel flow:

https://uofi.box.com/s/udjqeq3k74hncathbhybtqhdzpqtnyas

Flow around a sphere is a more direct case because there is a strong anomaly.

Drag Reduction and Drag Enhancement

Toms, B. A. “Some observations on the flow of linear polymer solutions through straight tubes at large Reynolds number,” Proc First Int Congr on Rheol II:135– 141 (1948)

White, A., “Effect of polymer additives on boundary layer separation and drag of submerged bodies,” Nature 211, 1390 (1966)

The JA-relation gives the necessary and sufficient conditions for drag reduction and for drag enhancement! The mean drag is directly related to the mean vorticity flux

$$-\langle \mathbf{F} \rangle \cdot \mathbf{V} = -\frac{1}{2} \int dJ \int \epsilon_{ijk} \langle \Sigma_{ij} \rangle d\ell_k$$

which in turn is related to (generalized) enthalphy gradients

$$\langle \Sigma_{ij} \rangle = \epsilon_{ijk} \partial_k \langle h \rangle$$

Drag can be reduced <u>only</u> by reducing the cross-stream flux of spanwise vorticity, and drag can be enhanced <u>only</u> by increasing that flux. We urge focused empirical investigation of the vorticity flux in drag-reduced and drag-enhanced flow.

Drag Reduction and Drag Enhancement

Toms, B. A. “Some observations on the flow of linear polymer solutions through straight tubes at large Reynolds number,” Proc First Int Congr on Rheol II:135– 141 (1948)

White, A., “Effect of polymer additives on boundary layer separation and drag of submerged bodies,” Nature 211, 1390 (1966)

The JA-relation gives the necessary and sufficient conditions for drag reduction and for drag enhancement! The mean drag is directly related to the mean vorticity flux

$$-\langle \mathbf{F} \rangle \cdot \mathbf{V} = -\frac{1}{2} \int dJ \int \epsilon_{ijk} \langle \Sigma_{ij} \rangle d\ell_k$$

which in turn is related to (generalized) enthalphy gradients

$$\langle \Sigma_{ij} \rangle = \epsilon_{ijk} \partial_k \langle h \rangle$$

Drag can be reduced <u>only</u> by reducing the cross-stream flux of spanwise vorticity, and drag can be enhanced <u>only</u> by increasing that flux. <u>We urge focused empirical investigation of the vorticity flux in drag-reduced and drag-enhanced flow.</u>

An Experimental Puzzle on Anomalous Dissipation

PHYSICAL REVIEW E VOLUME 56, NUMBER 1 JULY 1997

Energy injection in closed turbulent flows: Stirring through boundary layers versus inertial stirring

O. Cadot,* Y. Couder, A. Daerr, S. Douady, and A. Tsinober†
Laboratoire Physique Statistique, Ecole Normale Supérieure, 24 rue Lhomond, 75231 Paris, France

strong anomaly: flow past a grid, jets through orifices, wakes behind bluff bodies such as cylinders and spheres

weak anomaly: pipe and channel (Poiseuille) flow, developing boundary layer over a flat plate, Taylor-Couette flow, von Kármán flow (or “French washing machine”), Rayleigh-Bénard turbulence…*.except when the walls are rough!*

What is common to all of the flows of the second class is that there is no form drag when the walls are smooth, but form drag appears with wall roughness.

An Experimental Puzzle on Anomalous Dissipation

3-D measurements of the flow around two roughness cubes

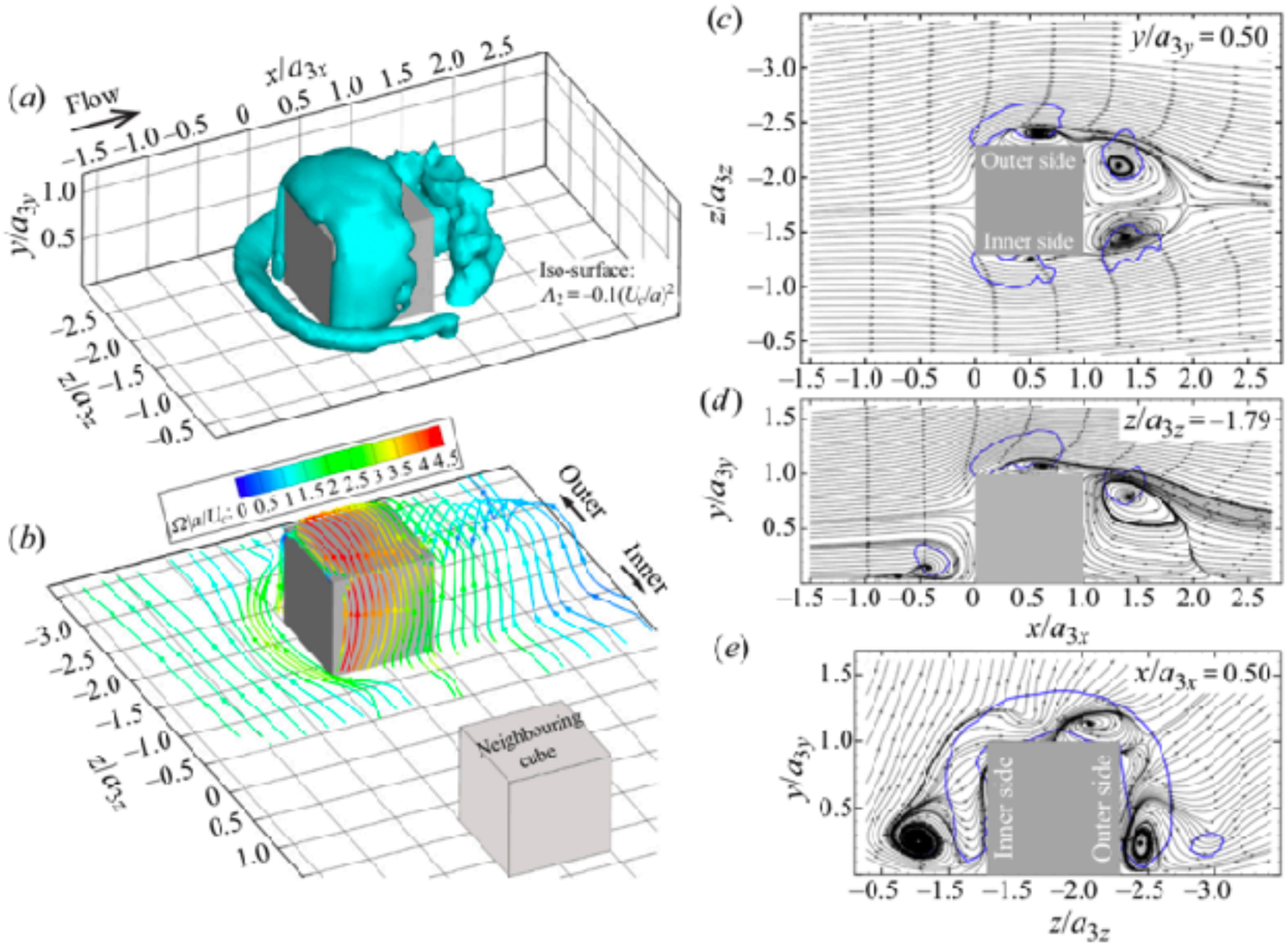

Figure 3. Characteristic primary flow structure around one of the cubes for $\lambda = 2.5a$. (*a*) Iso-surface of $\Lambda_2 = -0.1U_c^2/a^2$; and (*b*) vortex lines colour coded with the vorticity magnitude. (*c–e*) Selected in-plane streamlines: (*c*) *x*–*z* plane at $y/a_{3y} = 0.5$, (*d*) *x*–*y* plane at $z/a_{3z} = -1.79$ and (*e*) *y*–*z* plane at $x/a_{3x} = 0.5$. Blue lines: contour of $\Lambda_2 = -0.1U_c^2/a^2$ showing the intersections with the vortical canopy, arch-like and horseshoe vortices.

J. Gao, K. Agarwal and J. Katz, J. Fluid Mech. (2021), vol. 918, A31, doi:10.1017/jfm.2021.184

An Experimental Puzzle on Anomalous Dissipation

PHYSICAL REVIEW E VOLUME 56, NUMBER 1 JULY 1997

Energy injection in closed turbulent flows: Stirring through boundary layers versus inertial stirring

O. Cadot,* Y. Couder, A. Daerr, S. Douady, and A. Tsinober†
Laboratoire Physique Statistique, Ecole Normale Supérieure, 24 rue Lhomond, 75231 Paris, France

strong anomaly: flow past a grid, jets through orifices, wakes behind bluff bodies such as cylinders and spheres

weak anomaly: pipe and channel (Poiseuille) flow, developing boundary layer over a flat plate, Taylor-Couette flow, von Kármán flow (or "French washing machine"), Rayleigh-Bénard turbulence….except when the walls are rough*!*

What is common to all of the flows of the second class is that there is no form drag when the walls are smooth, but form drag appears with wall roughness.

Form drag described by the JA-relation appears necessary for a strong dissipative anomaly in 3D incompressible fluid turbulence, for laboratory flows.

Unity of Drag in Classical and Quantum Fluids

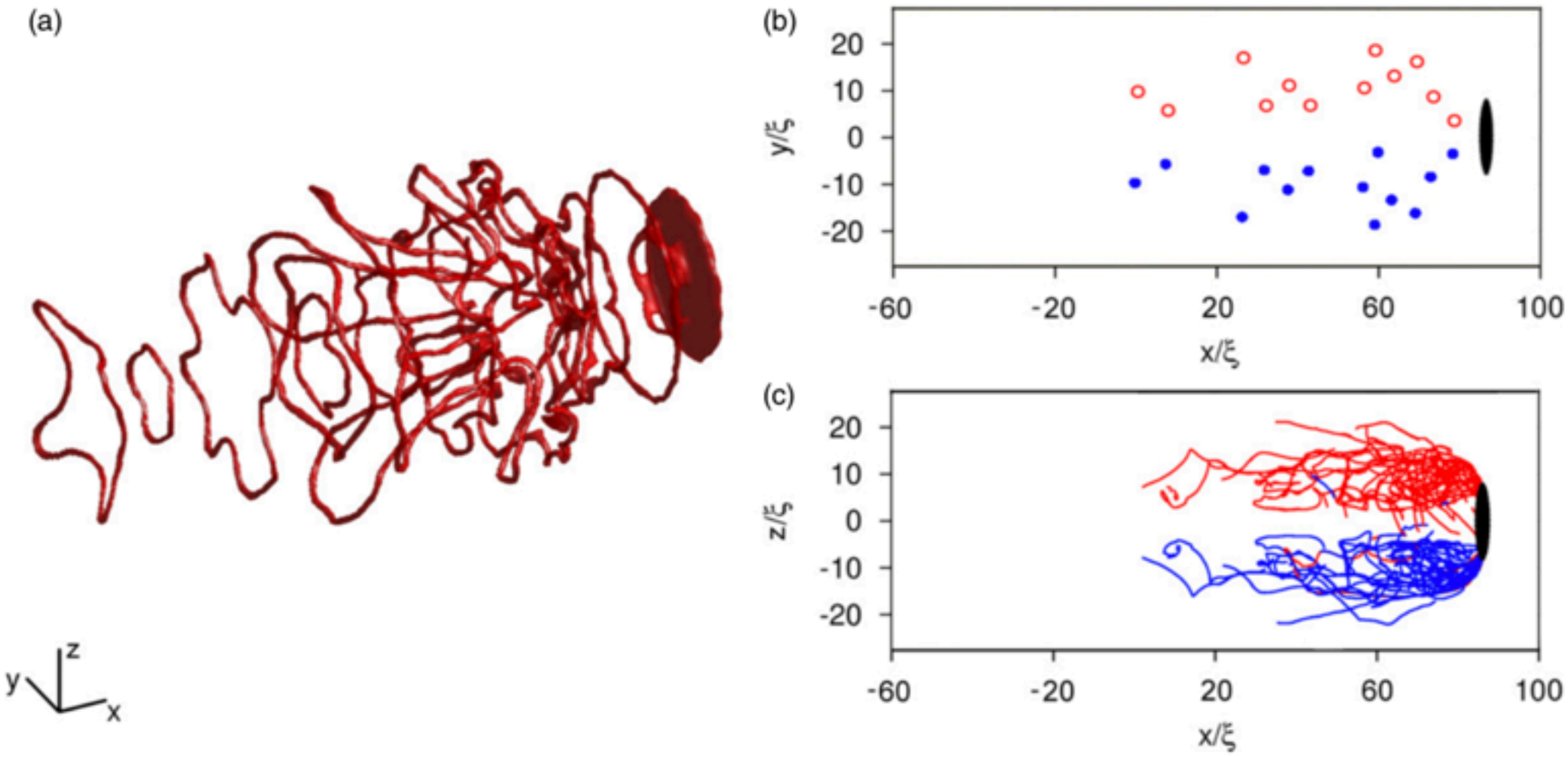

Figure 7. Symmetric wake in 3D at $t = 450(\xi/c)$ for an elliptical obstacle ($d = 5\xi$ and $\epsilon = 5$) moving at $v = 0.6c$. (a) Isosurface plot of low density, over a range [0, 100] in x and $[-25, 25]$ in y and z. (b) Vortex locations in the xy plane. (c) Vortex trajectories in the xz plane. Here (b) and (c) show opposing circulation in red and blue.

Detailed JA-Relation in Superfluid Turbulence?

Many studies of superfluid drag, starting with Frisch et al. (1992), use the model of Gross-Pitaevskii

$$i\hbar\frac{\partial\psi}{\partial t} = -\frac{\hbar^2}{2m}\boldsymbol{\nabla}^2\psi + g|\psi|^2\psi$$

Do our results hold there? Of course, the original Josephson-Anderson relation holds! With $\psi = \sqrt{n}e^{i\theta}$, then

$$\hbar\frac{d\theta}{dt} = -\left(\mu + \frac{1}{2}m|\mathbf{u}|^2\right)$$

with chemical potential μ and superfluid velocity $\mathbf{u}$ given by

$$\mu = gn - \frac{\hbar^2}{2m}\frac{\boldsymbol{\nabla}^2\sqrt{n}}{\sqrt{n}} \qquad\qquad \mathbf{u} = \frac{\hbar}{m}\boldsymbol{\nabla}\theta \ .$$

Taking a gradient gives the Josephson-Anderson relation in differential form

$$m\frac{\partial\mathbf{u}}{\partial t} = -\boldsymbol{\nabla}\left(\mu + \frac{1}{2}m|\mathbf{u}|^2\right) + m\kappa_v\mathbf{v}_v\times\hat{\mathbf{z}}\,\delta^2(\mathbf{r}-\mathbf{r}_v(t))$$

where $\kappa_v = \pm\dfrac{h}{m}$ is the circulation of a vortex line pointing in the z-direction at the position $\mathbf{r}_v(t)$ and moving with velocity $\mathbf{v}_v = d\mathbf{r}_v/dt$.

Detailed JA-Relation in Superfluid Turbulence?

The Gross-Pitaevskii equation is equivalent to the *quantum Euler equations*

$$\partial_t \rho + \boldsymbol{\nabla}\cdot(\rho \mathbf{u}) = 0$$

$$\partial_t (\rho \mathbf{u}) + \boldsymbol{\nabla}\cdot(\rho \mathbf{u}\mathbf{u}) = -\boldsymbol{\nabla} p + \boldsymbol{\nabla}\cdot\boldsymbol{\Sigma}$$

with mass density $\rho = mn$ and with pressure p and *quantum stress* $\boldsymbol{\Sigma}$ given by

$$p = \frac{g\rho^2}{2m^2}, \quad \boldsymbol{\Sigma} = \frac{\hbar^2}{4m}\triangle\rho\,\mathbf{I} - \frac{\hbar^2}{m^2}\boldsymbol{\nabla}\sqrt{\rho}\,\boldsymbol{\nabla}\sqrt{\rho}$$

This is a compressible fluid model! In fact, compressibility plays a crucial role in the drag phenomena observed for the GP-model, as evidenced by the fact that the critical velocity for vortex generation is some fraction of the sound speed.

Does the detailed Josephson-Anderson relation of Huggins extend to the Gross-Piataevskii model of a superfluid? Note that the GP model satisfies the Kelvin circulation theorem (e.g. Damski & Sacha, 2003) — as does barotropic Euler— and thus a potential flow solution may exist as a background “reference field”.

Relation with Stochastic Lagrangian Dynamics of Vorticity

We have previously discussed in this seminar the stochastic Lagrangian formulation of incompressible Navier-Stokes

https://uofi.box.com/s/7t3r0ohqpssjf10u3lmax19avchxv6no

in which the Kelvin theorem and Cauchy invariants of the incompressible Euler dynamics are preserved as stochastic conservation laws (martingales). Cf.

E. R. Huggins, “Dynamical theory and probability interpretation of the vorticity field,” Phys. Rev. Lett. 26, 1291-1294 (1971)

Recently, with Tamer Zaki and Mengze Wang, we have extended the stochastic Lagrangian approach to vorticity dynamics with the Lighthill source $\boldsymbol{\sigma}$ as the Neumann boundary conditions. We apply this method to determine the origin of the strongly magnified vorticity and viscous wall stress in turbulent wall-bounded flows, in particular at turbulent spots in a transitional zero pressure-gradient boundary layer. Stay tuned…!!!

The links between the Eulerian Josephson-Anderson relation and the stochastic Lagrangian approach to vorticity dynamics are obscure and remain to be understood!

That’s all, for now…

Thanks!!!